國立臺灣大學生物資源暨農學院園藝暨景觀學系

碩士論文

Department of Horticulture and Landscape Architecture
College of Bioresource and Agriculture
National Taiwan University

Master's Thesis

歐洲種及雜交種葡萄對乾旱逆境之光合作用生理反應

Photosynthetic physiology of vinifera and hybrid grapes in response to drought stress

柳沐真

Mu-Chen Liu

指導教授：李國譚 博士

Advisor: Kou-Tan Li, Ph.D.

中華民國 113 年 2 月

February, 2024

doi:10.6342/NTU202400535

致謝

首先感謝我的指導老師 李國譚老師的引導，一路從大學部到研究所帶我做研究，教我看到核心問題並解決。感謝口試委員 李金龍老師的鼓勵、 張哲嘉老師和 林宣佑老師細心指導修正論文的缺失之處。除此之外感謝盧老師(Tony)在前期回答我光合作用模擬相關的問題。謝謝四號館和花卉館的許多老師們從大學部到碩士班對我的照顧，每位老師的關心都給了我許多支持。

在園藝系受許多學長姐和學弟妹的幫助，謝謝法平學長指導我做光合模擬，學弟品睿教我使用儀器以及交接葡萄給我，還有士藝學長時不時捎來問候，以及嵐雁學姊的關心。謝謝這幾年間一起在研究室工作的大家：偉哲、揚曦、顥澄、越予、宣涵、偉俊、弘明、瑞琪、瑜寧和山森未來；大學部迦勒、冠廷、彰健、秉哲和禮恆的分擔。在這個研究室遇到太多人，沒唱到名的還請見諒，感謝大家的陪伴與打拼。

感謝從大學部一起走來的朋友們：靖媛、昀珊、珮綺、令儀，特別是大家的餵食和時不時把我拉門。高中的朋友芳瑜、宜家和鈺婷，每次的聚會我都很珍惜。慈幼義光的大家，特別是劉蘋和子欣的陪伴。謝謝女排和四號館動起來的大家，拉我出門運動。感謝一起勇闖英國的靖媛、薇涵和妮臻，在研究生涯的末尾、最迷惘的時候交換了很多想法；還有邱園的 Cheung 和 Richard，這段時間幫助我建立信心，讓我在研究中更敢於表達，也開闊我對植物學、園藝學相關研究的看法。

最後是我的家人們，家人是我最大的後盾，支持我讀書、做研究，包容我各種任性和脾氣。還有也很重要的自己，感謝你走得很慢，卻從未離開。

doi:10.6342/NTU202400535

摘要 (Chinese Abstract)

葡萄(*Vitis* spp.)為世界重要的園藝作物，主要的栽培種包括歐洲種(*V. vinifera*)，及其與美洲種(*V. labrusca*)的雜交種，後者因較適應亞熱帶地區潮濕的氣候，在臺灣廣泛栽培。歐美雜交種葡萄遺傳 *V. labrusca* 的特徵，如‘金香’以及‘黑后’葉片背面具有絨毛。絨毛影響葉片的氣體交換，並且被視為忍受乾旱逆境的特徵之一。本文探討‘麗絲玲’(*V. vinifera* ‘Riesling’) 與雜交種葡萄‘黑后’(‘Black Queen’)和‘金香’(‘Golden Muscat’)氣體交換差異，進一步比較不同程度乾旱逆境下之光合作用特徵，並將數據利用 *FvCB* 模型(Farquhar, von Caemmerer, and Berry biochemical model)進行擬合以得到葉肉細胞導度(mesophyll conductance, g_m)以及光合生化反應參數。在無水分逆境的環境下，‘麗絲玲’於二氧化碳濃度 400 μmol·mol^{-1} 之光合作用淨同化速率(net assimilation rate, A)以及氣孔導度 (stomata conductance, g_s)最高。水分利用效率(intrinsic water use efficiency, WUE_i)與 g_m /g_s 呈現正相關，‘金香’之 WUE_i 與 g_m /g_s 為三個品種中最高。利用數值積分方法(numerical integrated method)發現飽和光度最大電子傳遞能力(maximum electron transport capacity under saturating light, J_{max})為‘黑后’及‘金香’之 A 較‘麗絲玲’低的主要因子。為進一步了解 g_m 和 WUE_i 的關係，在不同程度的缺水進行第二個氣體交換測量分析試驗。利用氣孔導度區分不同的缺水程度，結果顯示三葡萄品種之 A, J_{max} 以及初始電子傳遞效率斜率(the initial slope of electron transport rate versus light, φ)皆隨著乾旱程度上升而下降，而 WUE_i 以及 g_m /g_s 在乾旱逆境中仍呈現正相關。‘金香’的 A 受乾旱之影響最小，且在極度乾旱時仍較‘麗絲玲’高。透過數值積分方法分析，擴散性因子(diffusional factors, g_s 及 g_m)為兩個雜交種葡萄在乾旱逆境下光合作用效率下降的主要原因，但在‘麗絲玲’中則非主因。但極度乾旱時，g_m 則是雜交種葡萄維持較‘麗絲玲’高的光合同化效率之主因。觀察葉背絨毛以及氣孔密度，結果顯示‘金香’具有最高的絨毛密度，和 WUE_i 以及耐旱程度一致。本試驗顯示‘黑后’及‘金香’雜交種葡萄不僅具較高絨毛密度，且在缺水逆境下能夠透過維持 g_m 以及 WUE_i，故較‘麗絲玲’良好的抗乾旱能力。

關鍵字：*FvCB* 模擬，葉肉細胞導度，飽和光度最大電子傳遞能力，數值積分方法

doi:10.6342/NTU202400535

Abstract

Grapes (*Vitis* spp.) are one of the most important horticultural crops worldwide. Commercial cultivars are mainly derived from the European grape, *V. vinifera* and its hybrids with American grape, *V. labrusca*. The hybrid grapes are widely cultivated in Taiwan and other subtropical regions, due to their better tolerance to humid climates. The hybrid cultivars 'Golden Muscat' and 'Black Queen' inherited the leaf abaxial trichomes from *V. labrusca*. The leaf trichome may affect leaf gas exchange and has been identified as an indicator of drought tolerance. This thesis aimed to reveal the gas exchange differences between 'Golden Muscat', 'Black Queen' and *V. vinifera* 'Riesling' and their responses to drought. In this study, light response and CO_2 response (A-C_i) curves of gas exchange behaviors of potted vinifera 'Riesling' and two hybrid cultivars, 'Black Queen' and 'Golden Muscat' vines were measured at air temperature 25℃. Data were fitted to a modified Farquhar, von Caemmerer, and Berry biochemical model (*FvCB*) to estimate mesophyll conductance (g_m) and biochemical parameters. In the first experiment, gas exchange at ambient CO_2 concentration (C_a, 400 μmol·mol^{-1}) was measured under well-watered condition. The results showed that 'Riesling' exhibited the highest net assimilation rate (A) and stomata conductance (g_s). Water use efficiency (WUE_i) was positive related to g_m /g_s, which 'Golden Muscat' had the highest intrinsic water use efficiency (WUE_i) and g_m /g_s. The data were further analyzed with a numerical integration approach and the result showed that the biochemical factor maximum electron transport capacity under saturating light (J_{max}) was the major contributor to the lower A of the hybrid cultivars. In the second experiment, the effect of g_m on WUE_i, was investigated on vines subject to various drought indicated by g_s. The results showed that at ambient CO_2 concentration (C_a, 400 μmol·mol^{-1}), A, J_{max}, and the initial slope of electron transport rate versus light (φ) decreased in all three cultivars in

doi:10.6342/NTU202400535

vines suffering moderate drought stress. The positive relationship between g_m /g_s and WUEi was maintained under water deficiency. *A* of 'Golden Muscat' was less influenced by drought stress and superior then that of 'Riesling' at extreme water deficiency. the data were further analyzed using a numerically integrated method and the results showed that as the drought stress increased, diffusional factors (g_s and g_m) were the major contributors to the decrease in *A* in the two hybrid vines but had little influence in 'Riesling' vines. However, in the extreme drought stress, g_m was the main positive contributor maintaining a rather stable *A* of the two hybrids over 'Riesling'. The trichome densities were positive correlated to WUE_i, which 'Golden Muscat' was the highest of all. This thesis suggests hybrid cultivars have a better photosynthetic response to extreme water deficiency by maintaining g_m and WUE_i.

Keywords: *FvCB* model, mesophyll conductance, maximum electron transport capacity, numerical integration approach

doi:10.6342/NTU202400535

Table of contents

doi:10.6342/NTU202400535

doi:10.6342/NTU202400535

doi:10.6342/NTU202400535

List of Tables

doi:10.6342/NTU202400535

List of Figures

doi:10.6342/NTU202400535

doi:10.6342/NTU202400535

Chapter 1 Literature review and hypothesis

Introduction

Grapes (*Vitis* spp.) are one of the most important horticultural fruit crops in the world. The world's production reached 78 million tons in 2021 (FAO, 2021), and wine grapes accounted for 57% of that (OIV, 2019). In the wine grape industry, the major cultivated species is vinifera grape (*Vitis vinifera* L.), which originated in the Middle East and adapted to the dry summer weather in the Mediterranean region (Keller, 2010). The grape cultivars dominant in Taiwan are complex hybrids between vinifera grapes and American-derived species, which are adapted to humid summers (Yang, 2005). According to statistics from the Ministry of Agriculture in Taiwan (2021), the major varieties of wine grape in Taiwan were 'Golden Muscat' and 'Black Queen', which parents were vinifera grape and *V. labrusca* (Maul, 2023). Consequently, the hybrid cultivars have the leaf structure inherited from *V. labrusca*, with trichomes on the abaxial side. The trichome density on the lower side of the leaf varies among *Vitis* species (Keller, 2010). For instance, the trichome density of *V. vinifera* is less than 1 mm^{-2} on the leaf abaxial side, whereas that of *V. labrusca* is more than 1000 mm^{-2} (Kortekamp and Zyprian, 1999). This characteristic makes leaf hair density a specific identification marker in *Vitis* (Keller, 2010). Leaf trichomes provide grapes with physiological resistance to diseases such as downy mildew (Kono et al., 2018; Kortekamp and Zyprian, 1999), and affect the leaf gas exchange trait and water usage (Werker, 2000). In some plants, trichomes is also an indicator of stress tolerance. Drought tolerance has been brought to the attention of cultivation because of frequent extreme weather events (FAO, 2017). In this study, two hybrids 'Golden Muscat' and 'Black Queen' and one vinifera grape 'Riesling' were evaluate to determine the limiting factors in CO_2 assimilation by using gas exchange techniques. Second, their

doi:10.6342/NTU202400535

responses under water stress were examined to gain insight into leaf water and gas usage.

1.2. Photosynthesis response of grapes under water stress

1.2.1. Gas exchange of grapes in response to drought

As photosynthesis provides the materials for plant growth, it is an important index of plant growth, crop yield and stress response (Farquhar and Sharkey, 1994). The net assimilation rate (A) of grape leaves is greatly affected by water availability. As the irrigation of grapes stopped, stomatal conductance (g_s) and A decreased in both potted and field-grown grapes (Bota et al., 2001; Da Silva et al., 2017; Flexas et al., 2009; Flexas et al., 1999). A reduction in g_s from 0.5 mol·m^{-2}·s^{-1} resulted in a decline of A from 15 μmol·m^{-2}·s^{-1} as the soil water content decreased (Flexas et al., 2002). Additionally, transpiration rate (E) also decreased from 5 mmol·m^{-2}·s^{-1} to 1 mmol·m^{-2}·s^{-1} (Flexas et al., 1999). Decreases in A, g_s, and E have also been observed as irrigation was restricted for several days (Chaves et al., 2007; Martinez-Luscher et al., 2015; Patakas et al., 2005). Moreover, during the growing season, non-irrigated or irrigation-restricted grapes showed lower A, g_s and E than well-irrigated grapes (Tzortzakis et al., 2020; Zufferey et al., 2017). Following g_s, CO_2 concentration in the intercellular space (C_i) and at the carboxylation site (C_c) decreased as the soil water content decreased (Martinez-Luscher et al., 2015; Tzortzakis et al., 2020). However, in some cases, C_i was not significantly lower under drought stress in comparison to well-watered condition (Salazar-Parra et al., 2015). C_i showed a wide range from 270 μmol·m^{-2}·s^{-1} to 90 μmol·m^{-2}·s^{-1} as g_s decreased to 0.05 mol·m^{-2}·s^{-1} (Flexas et al., 2002). This variation in C_i resulted in the restriction of mesophyll conductance (g_m) to leave gas exchange (Flexas et al., 2002).

doi:10.6342/NTU202400535

g_m is often used to describe the efficiency of CO_2 diffusion from the intercellular space to the carboxylation site in a leaf. As water supply stopped, g_m decreased with g_s (Flexas et al., 2002). In grapes, g_m stayed at around 0.17 μmol·m^{-2}·s^{-1} in the beginning of drought stress and then started to decrease to around 0.05 μmol·m^{-2}·s^{-1} as drought occurred for several days (Flexas et al., 2009; Perez-Martin et al., 2009). Mesophyll resistance, the reciprocal of g_m, was doubled in non-irrigation vines in the field at the end of the growing season (Zufferey et al., 2017). These results showed that drought stress not only affects g_s but also affects the CO_2 transportation in mesophyll. Changes in g_m versus g_s showed a positive relationship in grape vines under drought condition (Perez-Martin et al., 2009). Additionally, some cultivars displayed higher A and g_m when restricting g_s at 0.05 mol·m^{-2}·s^{-1}, which led to higher intrinsic water use efficiency (WUE$_i$, A/g_s) and the ratio of g_m to g_s (Tomás M. et al., 2014). Overall, the interaction between g_m and g_s was important in analyzing the A response to water deficiency.

1.2.2. Photosynthetic biochemical processes of grapes in response to drought

Not only gas transportation but also the biochemical processes involved in response to photosynthetic efficiency in grapes. Flexas et al. (2009) found that the maximum carboxylation rate (V_{cmax}) remained unaffected at around 250 μmol·m^{-2}·s^{-1} in the beginning of drought and higher than that of the well-watered vines at the third to seventh day of drought. The Rubisco carboxylation and day respiration rate of potted *V. labrusca* showed a decline after 12 days of non-irrigation (Da Silva et al., 2017). On the other hand, the electron transport rate calculated from chlorophyll fluoresce (J_f) showed a similar trend to g_m, i.e., little changed in the beginning and a declined after prolonged restriction of water supply (de Souza et al., 2005; Flexas et al., 2009). Moreover, the

doi:10.6342/NTU202400535

carboxylation efficiency, which was analyzed by the initial slope of the A-C_c curve, remained unchanged until severe drought (Flexas et al., 2002). However, the decline in biochemical factors was not always found under drought conditions. Perez-Martin et al. (2009) revealed that V_{cmax} was not different between vines grown in well-irrigated and those in half field water capacity soils. Meanwhile, keeping the water availability at 40% of pot water capacity, V_{cmax} and J_{max} were unaffected after 10 and 20 days of treatment (Salazar-Parra et al., 2012). These diverse responses of biochemical processes emphasize the impact of biochemical process to photosynthetic response under drought.

1.2.3. Variability in the photosynthetic responses of grape cultivars to water deficiency

The photosynthetic strategies of the grapevines differed among cultivars. Bota et al. (2001) studied the gas exchange response of 20 local cultivars and two widespread cultivars of *V. vinifera* after irrigation was stopped and soil moisture was reduced to 60% of the well-watered condition. Their results showed that even with the same predawn water potential at drought condition, some cultivars maintained g_s and A as high as those in well-watered condition, whereas the other cultivars reduced g_s by over 40% in comparison to that of well-watered condition (Bota et al., 2001). Florez-Sarasa et al. (2020) studied the photosynthetic response of the local and wide-spread cultivars. Under drought conditions, the local cultivars had a A of 9.08 μmol·m^{-2}·s^{-1} and the widespread cultivar 'Merlot' had a A of 5.14 μmol·m^{-2}·s^{-1}. On the other hand, A of the hybrid cultivar 'Red Double Tase' decreased from 7.5 μmol·m^{-2}·s^{-1} to 1.5 μmol·m^{-2}·s^{-1} as the relative soil water content dropped from 85% to 65%. In contrast, A of the vinifera grape 'Cabernet Sauvignon' only decreased from about 4.5 μmol·m^{-2}·s^{-1} to 3.0 μmol·m^{-2}·s^{-1} (Guan et al., 2004). On the other hand, C_i showed a different trend in the two

doi:10.6342/NTU202400535

cultivars, which maintained high in ‘Red Double Tase’ but decreased in ‘Cabernet Sauvignon’ under slight drought conditions (Guan et al., 2004). These diverse responses of biochemical processes emphasize the need to understand the impact of water stress on photosynthetic efficiency.

1.2.4. Effect of trichomes to leaf water use and gas exchange

Cultivars derived from hybridization between *V. vinifera* and *V. labrusca* often have abaxial trichomes inherited from *V. labrusca*. Trichomes are modified single or multiple epidermal cells that make the plant surface hairy (Werker, 2000). Depending on their structure, the functions of trichomes include secreting plant secondary metabolites by glandular trichomes and providing physiological protection to plants from pathogens and light by non-glandular trichomes (Werker, 2000). Leaf trichomes also influence gas exchange characteristics, with high density thickening the boundary layer of the leaf and decreasing the incident light to the leaf surface, whereas low density may cause greater air turbulent, increasing CO_2 uptake and water loss through transpiration (Schreuder et al., 2001; Schuepp, 1993). For example, pubescent trichomes protect leaves from intense incident light and lower *A* in *Encelia farinosa* (Ehleringer et al., 1976). The transpiration rate of *Wigandia urens* leaves with trichomes was lower than that of smooth leaves (Perez-Estrada et al., 2000). However, pubescent milkweed species (*Asclepias* spp.) showed higher *A* than glabrous species (Agrawal et al., 2009). In *Metrosideros polymorpha* and *Tillandsia* spp., although the gas exchange resistance of leaf trichomes and boundary layers increased in pubescent leaves, the influence was relatively small (Amada et al., 2017; Benz and Martin, 2006). In grapes, the trichomes were mostly determined to be resistant to downy mildew and other fungal diseases (Kono et al., 2018; Kortekamp and Zyprian, 1999), but their effect on gas exchange was

doi:10.6342/NTU202400535

less studied.

Although the direct influence of trichomes on gas exchange is still under investigation, some relationships exist between trichomes and leaf water use and stress tolerance. In olive (*Olea europaea* L.) and potato *(Solanum tuberosum* L.), the cultivars exhibited better drought tolerance with higher leaf trichome density than the susceptible species (Boguszewska-Mańkowska et al., 2018; Boughalleb and Hajlaoui, 2011). In tomato (*Solanum lycopersicum*), the density of leaf trichome and the ratio of trichome to stomata were positively related to the intrinsic water use efficiency (WUE_i) (Galdon-Armero et al., 2018). In the tropical rainforest, the canopy and emergent trees that are taller than the surroundings showed a positive relationship between WUE_i and trichome density (Ichie et al., 2016). Kenzo et al. (2008) reported that removal of the leaf trichome from *Mallotus macrostachyus* decreased WUE_i. In olive (*Olea europaea* L.) and *Wigandia urens*, leaf trichomes provided a protective layer against water loss, and cultivars with better water stress tolerance increased the number of trichomes on leaves when drought occurred (Boughalleb and Hajlaoui, 2011; Ennajeh et al., 2010; Guerfel et al., 2009; Perez-Estrada et al., 2000). This had also been observed in silver birch, and the increase in trichome density was especially on the abaxial side, suggesting that trichomes are an indicator of drought tolerance (Thitz et al., 2017). The hybrid cultivars of *V. labrusca* had higher trichome densities on the leaf back and were more adapted to the environment in Taiwan, which might have made them have a better response to drought.

doi:10.6342/NTU202400535

1.3. Modelling leaf gas exchange

1.3.1. Farquhar, von Caemmerer, and Berry (*FvCB*) model

Gas exchange measurements and the derived models have been widely used for investigating plant leaf photosynthesis processes. Farquhar, von Caemmerer, and Berry (1980) developed a model (*FvCB*) to describe biochemical processes of photosynthesis. This model separates photosynthetic assimilation rate (A) into two processes: Rubisco carboxylation and RuBP (ribulose-1,5-bisphosphate) regeneration. After that, Sharkey (1985) added the third process, triose phosphate utilization. Therefore, the final A is determined by the limitations of these three processes. Under the limitation state, the processes described by the photosynthetic properties are shown in the following formulas (1) to (3), respectively.

$$A_{\mathrm{c}} = \frac{V_{\mathrm{cmax}}\left(C_{\mathrm{c}} - \Gamma^{*}\right)}{C_{\mathrm{c}} + K_{\mathrm{C}}\left(1 + \frac{O}{K_{\mathrm{O}}}\right)} - R_{\mathrm{d}} \quad (1)$$

$$A_{\mathrm{j}} = \frac{J\left(C_{\mathrm{c}} - \Gamma^{*}\right)}{4C_{\mathrm{c}} + 8\Gamma^{*}} - R_{\mathrm{d}} \quad (2)$$

$$A_{\mathrm{p}} = 3\mathrm{TPU} - R_{\mathrm{d}} \quad (3)$$

where A_{c}, A_{j}, and A_{p} represent as limitation in Rubisco carboxylation, RuBP regeneration, triose phosphate utilization phases, respectively, to photoassimilation. Γ^{*} is the CO_2 compensation point in the absence of photorespiration; K_{C} and K_{O} are the catalytic constants for the carboxylation and oxygenation reactions of Rubisco; O is the mole fraction of O_2 at the carboxylation site; and TPU is the rate of phosphate release in triose phosphate utilization. By fitting the CO_2 response curve to this model, the maximum rate of Rubisco at the carboxylation site (V_{cmax}), the photosynthetic electron transport rate (J), the day respiration rate (R_{d}), and the CO_2 concentration at the carboxylation site (C_{c}) can be obtained, where C_{c} is calculated as formula (4),

$$C_{\mathrm{c}} = C_{\mathrm{i}} - \frac{A_{\mathrm{c}}}{g_{\mathrm{m}}} \quad (4)$$

doi:10.6342/NTU202400535

where C_i is the intercellular CO_2 concentration, and g_m is the mesophyll conductance.

Followed the original *FvCB* model, other modified models and methods have been published to obtain additional biochemical parameters in the photosynthesis process. The following modified equation (Caemmerer, 2000) describes the relationship between J and photosynthetic photon flux (PPF, I_{inc}):

$$J = \frac{J_{max}+\varphi I_{inc}-\sqrt{(J_{max}+\varphi I_{inc})^2-4\theta J_{max}\varphi I_{inc}}}{2\theta_j} \quad (5)$$

where φ is the initial slop of the relationship between J and I_{inc}, θ is the convexity factor, and J_{max} is the maximum electron transport rate.

By fitting the data of A versus I_{inc} to this equation and adjusting φ and θ to fit the J calculated from A in equation (2), the J_{max} at saturated light can be estimated. other methods combining the gas exchange with simultaneous chlorophyll fluoresce measurement provide additional information on the relationship between the electron transport rate and carbon assimilation (Caemmerer, 2000). Genty et al. (1989) proposed an approach to calculating electron transport rates from chlorophyll fluoresce (J_f), described as equations (6) and (7).

$$J_f = \alpha\beta I_{inc}\phi_{PSII} \quad (6)$$

$$\phi_{PSII} = 1 - \frac{F_s}{F_{m'}} \quad (7)$$

where J_f is closely correlated with J calculated by rearranging equation (2) from the CO_2 assimilation (Genty et al., 1989). This relationship allows the estimation of some parameters other than the gas exchange measurement.

1.3.2. Estimation of the *FvCB* parameters

In consideration of the influence of g_m on V_{cmax} and J, it is advised to estimate g_m

doi:10.6342/NTU202400535

rather than assume an infinite g_m (Sharkey, 2016; Sun et al., 2014). Though it is possible to estimate g_m directly by replacing C_c in equation (4) into (1) and (2), it is recommended to use methods combined with carbon isotope discrimination or chlorophyll fluorescence if available (Pons et al., 2009). The carbon isotope discrimination method was first used by Evans et al. (1986), based on the fractionation of ^{13}C measured simultaneously with gas exchange. The drawback of this method is that it is equipment-intensive (Sharkey et al., 2007). There are two methods to estimate g_m by combining gas exchange measurement with chlorophyll fluoresce: the constant J method and the variable J method (Harley Peter C. et al., 1992; Loreto et al., 1992). The chlorophyll fluoresce method was preferred for its availability compared with the carbon isotope method, but it still has a drawback in that the measurable leaf area is relatively small, which may cause leaks of the gas as measured (Pons et al., 2009). Moreover, the estimation of J_f relies on the exact estimates of α and β in the variable J method (Caemmerer, 2000). To solve this problem, Moualeu-Ngangue et al. (2017) introduced a modified fitting process by estimating $\alpha\beta$ simultaneously, which was used in this thesis study.

In addition to g_m, R_d is also recommended to be estimated separately to reduce the uncertainty of fitting too many parameters at the same time. There are three methods to estimate R_d: Kok (1948), Laisk (1977), and Yin et al. (2009) methods. Kok (1948) published a method based on the linear correlation of A to light at low irradiance, in which R_d is the intercepted value of A versus light regression line. Laisk (1977) estimated R_d by the intersection point of A-C_i curves under various light intensities, where the fixed CO_2 was photorespiration and the CO_2 released was R_d. The drawback of the Laisk's method is that the measurement was done under low C_i, which requires

doi:10.6342/NTU202400535

correcting the CO_2 leakage of the leaf chamber. Yin et al. (2009) also published a method using the light curve combined with chlorophyll fluoresce, which estimates R_d by the interception of the linear regression between A and $I_{inc}\phi_{PSII}/4$ at low light conditions. Yin's method considers the difference of ϕ_{PSII} at low light, thus having a wider range of data and yielding a better estimation of R_d compared to Kok's method (Yin et al., 2011). This thesis used chlorophyll measurements to estimate g_m; therefore, this thesis also used Yin's method to estimate R_d.

1.4. Analyze the limitations and contribution of individual variables to photosynthesis

As the parameters of the photosynthetic process can be calculated, attention had been drawn to identifying the limitations and quantifying the contribution of individual parameters to variations in A. Farquhar and Sharkey (1982) proposed a simple method to identify the stomatal limitation by modeling the A-C_i curve. On a given A-C_i curve where stomata limitation existed, C_i was lower than ambient CO_2 concentration (C_a) because CO_2 diffusion was resisted by stomata. As a result, if CO_2 had no obstacle, A without any limitation could be obtained from where C_a equals C_i on the A-C_i curve. The stomatal limitation (l_s) can be demonstrated by the following equation:

$$l_s = \frac{A' - A}{A'} \quad (8)$$

where A' is the non-limited A.

Similarly, the limitation of mesophyll(l_m) can also be calculated with the A-C_c curves, where the limitation of mesophylls occurred when CO_2 diffused from the intercellular space to the carboxylation site. This method has been used to estimate the limitations of photosynthesis (Bernacchi et al., 2002; Olsovska et al., 2016; Silim et al.,

doi:10.6342/NTU202400535

2010). However, this method is only applicable to the diffusional limitation but unable to estimate the biochemical influence of photosynthesis. On the other hand, Jones (1985) developed a partial derivate method to partition the changes in A into the percent contribution of individual parameters. Grassi and Magnani (2005) modified this method by assuming that changes in A were the result of a combination of g_s, g_m, and biochemical factors. In the photosynthesis process under the light-saturated condition (Rubisco carboxylation stage), the partition changes of A_c are demonstrated by equation (9). Dividing dA_c by A_c to express the changes into relative terms is shown as (10):

$$dA_c = \left(\frac{\partial A_c}{\partial g_{sc}}\right) dg_{sc} + \left(\frac{\partial A_c}{\partial g_m}\right) dg_m + \left(\frac{\partial A_c}{\partial V_{cmax}}\right) dV_{cmax} \quad (9)$$

$$\frac{dA_c}{A_c} = S_L + M_L + B_L = l_s \cdot \frac{dg_{sc}}{g_{sc}} + l_m \cdot \frac{dg_m}{g_m} + l_b \cdot \frac{dV_{cmax}}{V_{cmax}} \quad (10)$$

Where S_L, M_L, and B_L refer to the contributions of g_s, g_m and V_{cmax} to A_c, l_s, l_m, and l_b are corresponding relative limitations, and g_{sc} is stomatal conductance to CO_2 (g_s/1.6). The relative limitations are displayed as follows (Jones, 1985; Wilson et al., 2000):

$$l_s = \frac{\frac{g_{tot}}{g_{sc}} \cdot \frac{\partial A}{\partial C_c}}{g_{tot} + \frac{\partial A}{\partial C_c}} \quad (11)$$

$$l_m = \frac{\frac{g_{tot}}{g_m} \cdot \frac{\partial A}{\partial C_c}}{g_{tot} + \frac{\partial A}{\partial C_c}} \quad (12)$$

$$l_s = \frac{g_{tot}}{g_{tot} + \frac{\partial A}{\partial C_c}} \quad (13)$$

$$\frac{1}{g_{tot}} = \frac{1}{g_{sc}} + \frac{1}{g_m} \quad (14)$$

where g_{tot} refers to the total conductance of CO_2 from the leaf surface to the carboxylation site. To apply this approach, Grassi and Magnani (2005) defined the changes of A as the relative changes between reference A and comparison A (denoted as R and C), where relative limitation (l) is approximated by the averages of the two points ($\bar{l}$).

doi:10.6342/NTU202400535

$$\frac{dA_c}{A_c} \approx \frac{A_{c,R}-A_{c,C}}{A_{c,R}} \quad (15)$$

$$\frac{A_{c,R}-A_{c,C}}{A_{c,R}} \approx \bar{l}_s\left(\frac{g_{sc,R}-g_{sc,C}}{g_{sc,R}}\right) + \bar{l}_m\left(\frac{g_{m,R}-g_{m,C}}{g_{m,R}}\right) + \bar{l}_b \cdot \frac{V_{max,R}-V_{max,C}}{V_{max,R}} \quad (16)$$

Chen et al. (2014) modified this method for non-saturated light conditions by replacing the A_c condition with A_j and including biochemical factors J_{max} and J. These methods have been widely used to distinguish the contributions of parameters to the photosynthesis process (Flexas et al., 2009; Galle et al., 2009). However, Buckley and Diaz-Espejo (2015) described how this method actually partial derivates the natural logarithms of A rather than A itself. Equation (10) is actually rewritten by $dA/A = d\ln A$, into:

$$d\ln A_c = l_s d\ln g_{sc} + l_m d\ln g_m + l_b d\ln V_{cmax} \quad (17)$$

This may result in a bias when performing the derivation of A. Therefore, Buckley and Diaz-Espejo (2015) introduced a numerical integration method that integrated equation (9) into the following term (18):

$$\int_R^C dA_c = \int_R^C \left(\frac{\partial A_c}{\partial g_{sc}}\right) dg_{sc} + \int_R^C \left(\frac{\partial A_c}{\partial g_m}\right) dg_m + \int_R^C \left(\frac{\partial A_c}{\partial V_{cmax}}\right) dV_{cmax} \quad (18)$$

The limits of the integration refer to reference and comparison points. Then, taking stomatal CO_2 conductance (g_{sc}) as an example, the integration could be approximated as :

$$\int_R^C \left(\frac{\partial A_c}{\partial g_{sc}}\right) dg_{sc} \approx \sum_{k=0}^{n-1} \left(\Delta A_c|_{g_m, V_{cmax}}^{k,k+1}\right) \quad (19)$$

where 'k and k+1' refer to the changes ΔA_c at constant g_m and V_{cmax}. Taking this concept into account, the contribution of variable x_j to A in percentage of reference A (A_R) was defined as the following equation:

doi:10.6342/NTU202400535

$$\rho_{xj} \equiv \frac{100}{A_{\mathrm{R}}} \cdot \sum_{k=0}^{n-1} \left[\delta A \middle| \delta x_j\right]_k^{k+1} \qquad (20)$$

Therefore, this method estimated the contribution of each variable to the overall *A* directly by the photosynthetic model, which could invite more parameters under multiple environments such as light intensity and temperature.

1.4.2. Photosynthetic limitation under drought

Flexas et al. (2009) showed that the main photosynthetic limitations of photosynthesis under stress were both g_s and g_m in *V. berlandieri* x *V.rupestris*. At the beginning of the water deficiency, g_s was the dominant limitation to photosynthesis. The limitation of g_m was raised later on and shared nearly the same as g_s did (Flexas et al., 2009). Wheat (*Triticum aestivum* L.) and tobacco (*Nicotiana sylvestris*) exhibited similar patterns, indicating the importance of g_m in gas exchange under drought (Galle et al., 2009; Olsovska et al., 2016). Grapes displayed a varied value of C_i under drought suggesting that the decrease in *A* was not only due to limitations imposed by the reduction of g_s (Flexas et al., 2002). However, the limitation of g_m might be affected by the environment, which showed the limitation effect of biochemical factors rather than g_m (Galle et al., 2009). Overall, the limitation of photosynthesis in water stress was not only caused by g_s;. Non-stomatal limitations such as biochemical processes also played a big role.

1.5. Objective and hypothesis

The grape industry in Taiwan is dominated by hybrid cultivars (*V. vinifera* x *V. labrusca*), which have denser trichomes on the leaf abaxial side than *V. vinifera*. Moreover, the reduction of photosynthesis in *V. labrusca* was due to mesophyll

doi:10.6342/NTU202400535

conductance (Patakas et al., 2003). As previously stated, these differences contribute to differences in gas exchange on diffusional factors and better leaf water use under drought conditions. To understand the difference in gas exchange between hybrid cultivars and *V. vinifera*, the gas exchange measurement was conducted on two hybrid cultivars, ‘Golden Muscat’ and ‘Black Queen’, and the vinifera grape ‘Riesling’ in the summer of 2021. Further, to understand the leaf water use under drought, the gas exchange measurement on drought stress was conducted on the three grape cultivars in spring 2022. The gas exchange parameters in both experiments were modeled to get *FvCB* variables by Sharkey (2016) and Moualeu-Ngangue et al. (2017), and then the contribution of each parameter to photosynthesis changes was analyzed by a numerical integration method (Buckley and Diaz-Espejo, 2015). The analysis of photosynthetic response can be an identification of drought tolerance cultivars for future breeding programs.

doi:10.6342/NTU202400535

Chapter 2. Materials and Methods

2.1. Plant materials

The vinifera grape (*Vitis vinifera*) 'Riesling' ('RS') and hybrid cultivars (*V. vinifera* x *V. labrusca*) 'Black Queen' ('BQ') and 'Golden Muscat' ('GM') were used in this study. The plant materials were 2-year-old self-rooted cuttings planted in 2.5 L pots in an plastic greenhouse at National Taiwan University, Taipei, Taiwan (121°E, 25°N, 15m altitude). The planting medium was a commercial mixture of peat moss, vermiculite, and perlite (King Root No. 3, King Root Gardening Co., Ltd.). The grapevines were trained into two canes and pruned every spring and summer. The buds on canes were forced to burst by 20% (v/v) 2-chloroethanol immediately after pruning. After forcing bud break, each pot was added 5g organic fertilizer and 2g Patentkali (K_2O 30%, MgO 10%, SO_3 44%, K+S Aktiengesellschaft, Germany). Plants were regularly irrigated and fertilized with 0.1% (v/v) No. 43 fertilizer (N:P:K=15:15:15) (Taiwan Fertilizer Co., Ltd.) once a week.

2.2. The leaf gas exchange behavior of hybrid and vinifera grapes

This study included two experiments: experiment 1 (Exp.1) compared the gas exchange behavior of the hybrids and vinifera grapes; experiment 2 (Exp.2) was the gas exchange behavior of the grapes at various water contents.

2.2.1. The leaf gas exchange behavior of hybrid and vinifera grapes under well-watered condition

In Exp.1, leaf gas exchange measurements were made in September 2021 (5 weeks after summer pruning). Three vines with more than10 leaves from each cultivar were randomly chosen for the measurement. The grapevines were watered to full soil water

doi:10.6342/NTU202400535

capacity in the evening before the measurements to maintain the well-water condition of the grapevines.

2.2.2. The leaf gas exchange behavior under drought

Leaf gas exchange measurements for Exp.2 were made in April and May 2022, 6 weeks after spring pruning. Three vomes with 10-15 leaves from each cultivar were randomly chosen for the measurement. The vines were watered the night before the measurement. Water supply was stopped after measuring the well-water condition, and gas exchange was measured every other day. As plants reached the water-deficient condition, which was indicated by a g_s decrease of over 20% compared to the well-water condition, the measurements were made every day due to the rapid decline in the medium water content. According to the gas exchange measurement, the water deficiency level that the grapevine encountered was divided into four groups by g_s. The g_s of the well-watered condition was used as the standard in each cultivar, g_s reduced less than 20% indicating slightly water deficiency (D1), reducing less than 50% indicating moderate water stressed (D2), and more than 50% indicating extreme stress (D3).

2.3. Gas exchange measurement

Leaf gas exchange behavior was measured using a potable infra-red gas exchange system (LI-6400, Li-Cor, Lincoln, Nebr, USA) equipped with a leaf chamber fluorometer (LI6400-40, Li-Cor, Lincoln, Nebr, USA). Three plants per cultivar were randomly chosen as repeats (n=3). However, in Exp. 2, the extreme stress (D3) of 'BQ' and 'RS' were 2 repeats because the *A* was too low to measure the curves. The measurements were taken on the 3rd to 5th fully expanded leaf, which had no disease

doi:10.6342/NTU202400535

spots or insect infestation. The measurements were made in the laboratory from 8:00 to 14:00 to avoid the unstable environment and the circadian rhythm. The temperature in the environment was 25-26 °C, with the leaf chamber set to 25 °C. During the measurement, the relative humidity in the leaf chamber was controlled at 50±10% by the desiccant scrolls. The light intensity was controlled by the LED light resource in LI6400-40, and the ratio of red light to blue light was 9:1.

Each measurement included the CO_2 response curve (A-C_i curve), the light response curve, and the simultaneous chlorophyll fluorescence. Before the measurement, the chosen leaf was clapped on the leaf chamber for 15 to 30 minutes with a light intensity set to 1200 μmol·m^{-2}·s^{-1} for light adaptation. The curves were measured by the functions "Flr A-Ci curve" and "Flr light curve" in an auto program in LI-Cor OPEN 5.3.2 system. The CO_2 response curves were measured at 300 μmol·s^{-1} flow rate, and 1200 μmol·m^{-2}·s^{-1} light intensity. The series of ambient CO_2 concentrations (C_a) were: 400, 300, 200, 0, 100, 250, 400, 400, 600, 800, 1000, 1200, 1500 μmol·mol^{-1}. The two 400 μmol·mol^{-1} in the middle of the series was set to make more adaptation time for leaves as Ca increase. The light curves were measured at 300 μmol·s^{-1} flow rate, and 400 μmol·mol^{-1} CO_2 concentration. The series of light intensities in Exp.1 were: 1200, 900, 700, 500, 300, 200, 150, 100, 70, 50, 40, 30, 10, 0 μmol·m^{-2}·s^{-1}. To obtain a clear light saturation point in Exp. 2, the light incident series from 1200 to 200 μmol·m^{-2}·s^{-1} were adjusted into 1200, 900, 600, 400, 300, 200 μmol·m^{-2}·s^{-1}. The waiting time for every point on the curves was set to 3-5 minutes. The parameters including net assimilation rate (A), stomata conductance (g_s), intercellular CO_2 concentration (C_i), transpiration rate, and intrinsic water use efficiency (WUE_i, A/g_s) were obtained from the C_a=400 points in the A-C_i curves (n=3).

doi:10.6342/NTU202400535

2.4. Leaf gas exchange model fitting

After data were collected from the gas exchange measurements, the curves were fitted with the Farquhar, von Caemmerer, and Berry (*FvCB*) model (Farquhar et al., 1980) and derived methods (Moualeu-Ngangue et al., 2017) to generate other photosynthetic parameters. The *FvCB* model describes photosynthesis with three processes: Rubisco carboxylation, RuBP (ribulose-1,5-bisphosphate) regeneration, and triose phosphate utilization. A was therefore determined by the minimal assimilation rate in the three processes, shown as equations 2.1-2.4.

$$A_{\mathrm{c}} = \frac{V_{\mathrm{cmax}}\left(C_{\mathrm{c}} - \Gamma^{*}\right)}{C_{\mathrm{c}} + K_{\mathrm{C}}\left(1 + \frac{O}{K_{\mathrm{O}}}\right)} - R_{\mathrm{d}} \quad (2.1)$$

$$A_{\mathrm{j}} = \frac{J\left(C_{\mathrm{c}} - \Gamma^{*}\right)}{4C_{\mathrm{c}} + 8\Gamma^{*}} - R_{\mathrm{d}} \quad (2.2)$$

$$A_{\mathrm{p}} = 3\mathrm{TPU} - R_{\mathrm{d}} \quad (2.3)$$

$$C_{\mathrm{c}} = C_{\mathrm{i}} - \frac{A_{\mathrm{c}}}{g_{\mathrm{m}}} \quad (2.4)$$

The photo assimilation rate is represented as A_{c}, A_{j}, and A_{p} as being limited in the Rubisco carboxylation, RuBP regeneration, and triose phosphate utilization phases, respectively. Γ^{*} is the CO_2 compensation point in the absence of photorespiration; K_{C} and K_{O} are the catalytic constants for the carboxylation and oxygenation reactions of Rubisco; O is the mole fraction of O_2 at the carboxylation site; and TPU is the rate of phosphate release in triose phosphate utilization. A list of the symbols was showed in table 2.1. As equation 2.4 showed, the CO_2 concentration at the carboxylation site (C_{c}) was generated by mesophyll conductance (g_{m}), C_{i} and A_{c}. By introducing C_{i} into the formulas, the maximum rate of Rubisco at the carboxylation site (V_{cmax}), the photosynthetic electron transport rate (J) and the day respiration rate (R_{d}) were obtained by fitting the A-C_{i} curve to this model.

doi:10.6342/NTU202400535

In this study, the CO_2 response curves were fitted for the g_m and V_{cmax} using the Microsoft Excel VBA published by Moualeu-Ngangue et al. (2017). This derived method uses equation 2.5 with chlorophyll fluorescence (J_f) to estimates J in equation 2.2, and rearranges equation 2.2 into 2.7 to estimate g_m.

$$J_f = \alpha\beta I_{inc}\varphi_{PSII} \quad (2.5)$$

$$\phi_{PSII} = 1 - \frac{F_s}{F_{m'}} \quad (2.6)$$

$$g_m = \frac{A(\tau I_{inc}\phi_{PSII} - 4(A+R_d))}{\tau I_{inc}\phi_{PSII}(C_i - \Gamma^*) - 4(C_i + 2\Gamma^*)(A+R_d)} \quad (2.7)$$

In equation 2.5, α represents the light absorptance of the photosystem; β is the partitioning factor between photosystem I (PSI) and photosystem II (PSII); I_{inc} is the light incident irradiance; and ϕ_{PSII} represents the photochemical yield of PSII, which is estimated from chlorophyll fluorescence measurement (equation 2.6). F_s is the steady-state fluorescence, and F_m' is the maximal fluorescence during a saturating light flash. α and β were hard to estimate; thus, this method introduced τ=αβ to represent the fraction of light harvested by PSII in equation 2.7. Thereafter, A, C_i and φ_{PSII} of the A-C_i curve were input into Excel and solved to generate the fitting results of g_m and V_{cmax}. The C_a = 0 points in the curves were not included in the fitting process to reduce the instability of the fitting caused by equipment error at low C_a, as well as the C_a = 1500 points in some curves if the instability of that point lead to high sum of square error. The results of g_m there were influenced by C_i, thus, g_m in each repeat was obtained from the average of C_a =400.

As Moualeu-Ngangue et al. (2017) suggested, the day respiration rate (R_d) was generated separately in this study. The light intensity below 200 μmol·m^{-2}·s^{-1} in the light

doi:10.6342/NTU202400535

curve was used to generate R_d by Yin's method (Yin et al., 2011). The liner relation formula (equation 2.8) of A and $I_{inc}\phi_{PSII}/4$ was calculated by the Microsoft Excel liner regression function, and the intercept was R_d.

$$A = s(I_{inc}\phi_{PSII}/4) - R_d \quad (2.8)$$

After g_m and R_d were obtained, the two parameters were used in the fitting process of the light curve. The maximum electron transport rate (J_{max}), initial slope of electron transport rate versus light (φ) and the convexity factor of electron transport rate versus light (θ) were obtained by fitting the light curves into the Microsoft Excel VBA published by Sharkey (2016). This method is based on the J estimated from equation 2.9, and the inputs were A, C_i and light intensity of the light curve. Then fitting the J with calculated J from equation 2.2 by adjusting the variables φ, θ and J_{max}.

$$J = \frac{J_{max}+\varphi I_{inc}-\sqrt{(J_{max}+\varphi I_{inc})^2-4\theta J_{max}\varphi I_{inc}}}{2\theta} \quad (2.9)$$

All the variables were adjusted to leaf temperature 25℃ by equation 2.10 published by Harley P. C. et al. (1992),

$$\text{Adjust parameter} = \frac{e^{\left(c-\frac{\Delta H}{R\cdot T_k}\right)}}{1+e^{\left(\Delta S\cdot T-\frac{\Delta H_d}{R\cdot T_k}\right)}} \quad (2.10)$$

Where c is a scaling constant, ΔH_a is an enthalpy of activation, ΔH_d is enthalpy of deactivation and ΔS is entropy. R is molar gas constant (8.314 J·mol^{-1}·K^{-1}) and T_k is the leaf temperature in Kelvin (0°C = 273.15 K). To obtain the adjust variables, the variables in the measuring leaf temperature were divided by the adjust parameter in Appendix 1. Greer (2018) have reported that Kinetic constants of tobacco (Walker and Ort, 2015) fit well with the Chardonnay and Merlot grape leaves in the photosynthesis modeling processes, thus, K_o, K_c and Γ^* were adopted from tobacco to all of the fitting

doi:10.6342/NTU202400535

processes in this experiment, which were also showed in Appendix 1.

2.5. Contribution of the variables to the change of the *A*

To understand the impact of variables on A, the parameters include g_s, g_m, J_{max}, V_{cmax}, R_d, θ and ϕ were analyzed for their contribution to A changes. The average of the variables in each cultivar was analyzed by a numerical integration method (Buckley and Diaz-Espejo, 2015). Rather than a partial derivate of A, this method computed the contribution of the variables to the overall A directly:

$$\rho_{xj} \equiv \frac{100}{A_R} \cdot \sum_{k=0}^{n-1} \left[\delta A \middle| \delta x_j\right]_k^{k+1} \quad (2.11)$$

Where the contribution of variable x_j is expressed as ρ_{xj} (ρ[xj]) in percentage, which represents the variable that contributed to the difference of A between reference A (A_R) and comparison A. To estimate the CO_2 conductance, g_s was converted to stomatal CO_2 conductance (g_{sc}) by dividing g_s with 1.6 (the diffusion rate of CO_2).

The contribution of the variables can be divided into two groups: diffusional factors and biochemical factors. The contribution of diffusional factors is represented as ρ[DIFF], which is the sum of ρ[gsc] and ρ[gm]. The contribution of biochemical factors (ρ[BIO]) is the sum of ρ[Jmax], ρ[Vcmax], ρ[Rd], ρ[theta], and ρ[phi]. The contributions of boundary layer conductance (g_b) and O were neglected because they were constant in the leaf chamber. The contributions of Ko, Kc and Γ^* stayed at 0 because these variables were the same during the model fitting processes.

To understand the variables that caused the difference in A between the hybrid cultivars and vinifera grapes, the A_R in Exp. 1 was 'Riesling'. In Exp. 2, the A_R was not only set by 'Riesling' in the same water condition but also by the well-water condition

doi:10.6342/NTU202400535

in each cultivar to understand the water deficient stress response of the individual cultivar.

2.6. The soil water content

The soil water content (θ_g) of Exp. 2 was measured by a gravimetric method (Weil and Brady, 2017). The whole pot was weighted after every measurement (W_m). At the end of the experiment, the plants were took out of the pot and separate the roots form the media in the laboratory. The pot (W_c), fresh weight of the plant (W_p), and media (W_s) were separate and weighted. A sample of 50g of the media (W_{sam}) was collected and oven-dried at 105℃ for 24 hours (no more weight loss). After drying, the weight of the sample is represented as W_{sd}, and the water content at the end of the experiment is counted from equation 2.12. Therefore, the dry medium weight (W_d) of the potted plants was calculated by equation 2.13. Assume that the only weight loss during the measurements was caused by water loss; the water content during the measurements was calculated by equation 2.14.

$$\theta_g = \frac{W_{sam}-W_{sd}}{W_{sd}} \times 100\% \quad (2.12)$$

$$W_d = \frac{W_m}{1+\theta_g} \quad (2.13)$$

$$\theta_g = \frac{(W_w-W_p-W_f)-W_d}{W_d} \times 100\% \quad (2.14)$$

2.7. Trichome density

To understand the relationship between gas exchange behavior and trichome density, the leaves of three cultivars were observed (Johnson, 1975). Three plants in each cultivar were chosen randomly in October 2022 (8 weeks after summer pruning). In each pot, a leaf of the 3rd to 5th node was observed with the abaxial side under the

doi:10.6342/NTU202400535

dissecting microscope (Nikon SMZ-10, Nikon Co., Tokyo, Japan) with ocular lens of 10X and objective lens of 3X magnification. Every leaf was observed from 3 different site and recorded by the Canon EOS M100. Each sight was 44.5 mm^2. The trichomes were counted for number on the open-source software Inkscape, and the data was converted to per cm^2.

2.8. Stomata density

Stomata density was also observed in this study to better understand the impact of stomata density on photosynthetic behavior (Galdon-Armero et al., 2018). Due to the protruding vein and trichomes on the abaxial leaf side, the stomata were observed by a clearing technique (Vasco et al., 2014) rather than the impression method. Each cultivar selected one leaves from 3^{rd} to 5^{th} nod in 3 different pots (n=3). Before sampling, the trichomes of 'Golden Muscat' were picked off with tape and tweezers. For sampling, a 1 cm^2 square was cut from each leaf in 5 different locations away from secondary veins. These sample pieces were soaked in 95% ethanol in 20 ml vails and heated in boiling water. During the heating process, the ethanol was refreshed several times until it no longer changed color. Then the solution was replaced with 4% (v/v) NaOH and heated to 50°C. The NaOH solution was changed daily until the color no longer changed, which determined that the clearing process was done. 3 pieces of leaf tissue were observed by an optical microscope (Nikon, Nikon Co., Tokyo, Japan) with ocular lens 10X and objective lens 10X magnification. Pictures of the samples were taken, and the stomata were counted and labeled on the open-source software Inkscape. Each sight was 0.5 μm^2, and the data was converted to per μm^2.

doi:10.6342/NTU202400535

2.9. Data analysis

The results of gas exchange and modeling, soil water content, trichome density, and stomata density were analyzed for significance using ANOVA and the least significant difference test at $P<0.05$ in SPSS25. The mean and standard error were calculated using Microsoft Office Excel. To comprehend the relationship between the gas exchange variables and the *FvCB* variables, a Pearson correlation matrix and scatter graph for the correlation of the variables were also created in Excel. The data for the Pearson correlation were created from the repeats of each variable in Experiment 1 and from the means of the variables in Experiment. The mean gas exchange data from Experiment 1 were used to analyze the relationship with trichomes.

doi:10.6342/NTU202400535

Table 2.1. List of the symbols.

Symbol	Description
A	Net assimilation rate
C_a	Ambient CO_2 concentrations
g_s	Stomata conductance in H_2O
C_i	Intercellular CO_2 concentration
WUE_i	Intrinsic water use efficiency (A/g_s)
Γ^*	CO_2 compensation point in the absence of photorespiration
K_C	Catalytic constants for the carboxylation reactions of Rubisco
K_O	Catalytic constants for the oxygenation reactions of Rubisco
O	Mole fraction of O_2 at the carboxylation site
TPU	rate of phosphate release in triose phosphate utilization
C_c	CO_2 concentration at the carboxylation site
g_m	mesophyll conductance
V_{cmax}	the maximum rate of Rubisco at the carboxylation site
J	photosynthetic electron transport rate
R_d	day respiration rate
J_f	chlorophyll fluorescence electron transport rate
α	light absorptance of the photosystem
β	partitioning factor between PSI and PSII
I_{inc}	light incident irradiance
ϕ_{PSII}	photosystem II (PSII) electron transport efficiency
F_s	steady-state fluorescence
F_m'	the maximal fluorescence during a saturating light flash
τ	the fraction of light harvested by PSII (αβ)
J_{max}	the maximum electron transport rate
φ	initial slope of electron transport rate versus light
θ	convexity factor of electron transport rate versus light
ρ_{xj} (ρ[xj])	The contribution of the variable x_j to the difference of A
g_{sc}	stomatal CO_2 conductance
ΔH_a	enthalpy of activation
ΔH_d	enthalpy of deactivation
ΔS	entropy
θ_g	soil water content

doi:10.6342/NTU202400535

Chapter 3. Results

3.1. Gas exchange measurements of the hybrid and vinifera grape cultivars

3.1.1. Gas exchange behavior

To understand the gas exchange behavior of the hybrid and vinifera grapes, light curves (Fig. 3.1) and CO_2 response (A-C_i) curves (Fig. 3.2) in experiment 1 were measured under well-water condition. The light curves are shown in Fig. 3.1. The net assimilation rates (A) of the three cultivars were similar to each other at low light intensities. In the light intensity > 400 μmol·m^{-2}·s^{-1}, 'Riesling' ('RS') showed significantly higher A than the two hybrid 'Black Queen' ('BQ') and 'Golden Muscat' ('GM'). At saturating light intensity (photosynthetic photon flux density (PPFD) > 500μmol·m^{-2}·s^{-1}), A of 'RS' was around 10 μmol·m^{-2}·s^{-1}, while 'GM' and 'BQ' were at 6 μmol·m^{-2}·s^{-1}.

Fig. 3.2 displayed the A-C_i curves. At intercellular CO_2 concentration (C_i) above 200 μmol·mol^{-1}, the difference between 'RS' and hybrid cultivars in A was noticeable. A of 'RS' was 5 μmol·m^{-2}·s^{-1} at C_i = 200 μmol·mol^{-1} and climbed to 20 μmol·m^{-2}·s^{-1} at C_i = 1000 μmol·mol^{-1}. A of hybrid cultivars were 3 μmol·m^{-2}·s^{-1} at C_i=200 μmol·mol^{-1} and rose to 14 μmol·m^{-2}·s^{-1} at C_i=1000 μmol·mol^{-1}.

The gas exchange variables at 400 μmol·mol^{-1} ambient CO_2 concentration (C_a) were observed to understand the gas exchange behavior of the three cultivars at optimal temperature (25 ℃) and saturating light (Table 3.1). A of 'BQ' and 'GM' were 7.48 and 7.39 μmol·m^{-2}·s^{-1}, respectively, while that of 'RS' was 11.59 μmol·m^{-2}·s^{-1}, which was significantly higher than the hybrid cultivars. In addition to A, 'RS' had higher stomata conductance (g_s, 0.26mol·m^{-2}·s^{-1}) and transpiration rate (E, 4.36μmol·m^{-2}·s^{-1}) than the

doi:10.6342/NTU202400535

hybrid cultivars. ‘GM’ had the highest intrinsic water use efficiency (WUE_i, 68.65 μmol·mol^{-1}). Though ‘BQ’ had higher g_s than ‘GM’, it had A the same with ‘GM’. ‘BQ’ had lower g_s than ‘RS’ but similar C_i (307.58 μmol·mol^{-1}) at C_a=400 μmol·mol^{-1}. The photosystem II electron transport efficiency (ϕ_{PSII}) of the both hybrid cultivars were lower than ‘RS’. Vapor pressure deficiency based on leaf temperature (VPD) showed a significant difference between the three cultivars, with ‘RS’ having the lowest value of 1.71 kPa and ‘GM’ with 2.04 being the highest.

3.1.2. Farquhar, von Caemmerer, and Berry (*FvCB*) model fitting variables

The day respiration rates (R_d) of the three cultivars were similar to each other around 0.95 μmol CO_2 ·m^{-2}s^{-1} (Table 3.2). From the A-C_i curves, g_m and the maximum rate of Rubisco carboxylation (V_{cmax}) were derived by Moualeu-Ngangue et al. (2017), which were shows in Table 3.2. The fitting results of g_m showed a rather wide range, which led to non-significance amongst the three cultivars. ‘RS’ had V_{cmax} of 80.64 μmol·m^{-2}·s^{-1}, which was significantly higher than ‘GM’ (56.21 μmol·m^{-2}·s^{-1}), and ‘BQ’ was between them. The differences in φ and θ among the three cultivars were not significant (Table 3.2). While J_{max} was significantly different from ‘RS’ and the hybrid cultivars ‘GM’ and ‘BQ’, which reported values of 99.58, 64.30 μmol·m^{-2}·s^{-1}, and 53.40 μmol·m^{-2}·s^{-1}, respectively (Table 3.2).

3.1.3. The correlation between gas exchange and *FvCB* variables

The Pearson correlation between gas exchange and *FvCB* variables revealed positively linear correlations between A and g_s, E, g_m, and J_{max}, and negative correlations between A and θ (Table 3.3). C_i had a positive relationship with g_s and E. WUE_i and the ratio of g_m to g_s (g_m/g_s) were both substantially negatively correlated to C_i

doi:10.6342/NTU202400535

with correlation coefficients of -0.998 and -0.920, respectively. With a correlation coefficient 0.909, WUE_i demonstrated a linear relationship to g_m/g_s, highlighting the importance of g_m to leaf water use. Positive correlations existed between the biochemical processes J_{max} and V_{cmax} as well as J_{max}, θ and φ.

A and leaf water use were strongly correlated with g_m and g_m/g_s, despite the fact that there was no statistically significant difference in g_m between the three cultivars. The scatter graph (Fig. 3.3) demonstrated that 'RS' had a relatively high *A* with g_m even though g_m was not significantly different between the three cultivars. Although WUE_i did not have linear correlation to g_m, it was highly correlated to the g_m/g_s ratio. In comparison to the other two cultivars, 'GM' displayed a greater WUE_i at the same g_m/g_s ratio.

3.1.4. Contribution of the variables to the *A* difference on hybrid cultivars

To understand the photosynthetic differences between 'RS' and the hybrid cultivars, the *A* of 'RS' was used as the reference point for the numerical integrated method (Fig. 3.4). The results showed that the RuBP (ribulose-1,5-bisphosphate) regeneration process differentiated the differences in *A* among the three cultivars, and that V_{cmax} did not contribute to the variations in *A*. The result showed that *A* of 'BQ' was 41% and 'GM' was 37% lower than *A* of 'RS' (Fig. 3.1). The majority of the factors resulted in a negative change in *A* of the hybrid cultivars with the exception of θ, which made a positive change of 3% in 'BQ' and 1.5% in 'GM'. R_d also had a 0.5% slight beneficial influence in 'GM'. J_{max} of 'BQ' and 'GM' contributed 32% and 21%, respectively, to the less efficient *A* in comparison to 'RS'. The stomata conductance in CO_2 (g_{sc}, or $g_s/1.6$), and g_m also had a significant impact on the inferior *A* of the both

doi:10.6342/NTU202400535

hybrids. g_{sc} contributed 11% to the lower *A* in 'GM', while g_{sc} and g_m shared the similar impact in 'BQ'. In summary, *A* of 'BQ' was 41% lower than that of 'RS, with 11% contributed by the diffusional factors and 30% by the biochemical factors. A of 'GM' was 37% less efficient than that of 'RS', with 19% and 18%, respectively, contributed by biochemical and diffusional factors.

3.2. The gas exchange behavior of the hybrid and vinifera grape under various drought conditions

Table 3.4 displays the medium water content that the three cultivars underwent the various soil water availability. At the same level of stress, the medium water contents of the three cultivars did not significantly differ. The water content was over 100% under well-watered (WW) conditions and dropped to approximately 50% under slightly drought (D1) conditions. The water content continued to drop to approximately 30% under moderate drought (D2) conditions and reached approximately 25% under extreme drought (D3) conditions.

3.2.1. Gas exchange measurement under various drought conditions

The light curves of three cultivars at various drought conditions are depicted in Fig. 3.5. As the drought stress escalated, *A* of the three cultivars at the light saturated point declined. 'RS' had the greatest *A* of the three cultivars under WW conditions, measuring roughly 10 μmol·m^{-2}·s^{-1} at light intensities exceeding 500 μmol·m^{-2}·s^{-1}. In contrast, *A* of 'BQ' was the lowest (6 μmol·m^{-2}·s^{-1}). At D1, light saturated *A* for 'RS' reduced slightly to 8 μmol·m^{-2}·s^{-1} , whereas 'GM' fell to 6 μmol·m^{-2}·s^{-1}. At the moderate drought (D2) condition, light saturated *A* of the three cultivars dropped to 4 to 6 μmol·m^{-2}·s^{-1}, and 'GM' emerged as the cultivar with the greatest *A* among the three at

doi:10.6342/NTU202400535

saturating light. Three cultivars' *A* fell to 2 μmol·m^{-2}·s^{-1} at the extreme drought (D3).

The CO_2 response curves are shown in Fig. 3.6. Both C_i and *A* decreased with increasing drought stress. At the WW conditions, 'RS' had the highest *A* among the three cultivars at C_i = 1000 μmol·mol^{-1}. At stage D1, light saturated *A* of 'RS' reduced to about 15 μmol·m^{-2}·s^{-1}, which was comparable to 'GM'. From WW to D1, the saturated *A* of 'GM' did not decline. At D2, the highest C_i of the three cultivars dropped from 1200 μmol·mol^{-1} to roughly 900 μmol·mol^{-1}. In contrast to the other three stages, C_i was low at D3, and *A* was not stable. At D3, saturated *A* of the three cultivars dropped to 5 μmol·m^{-2}·s^{-1}.

Table 3.5 and Fig 3.7. shows the gas exchange behavior of the three cultivars under saturated light and C_a of 400 μmol·mol^{-1}. *A* of the three cultivars fell as drought stress increased, particularly in 'RS', which had a sharp decline from 10.66 μmol·m^{-2}·s^{-1} to 1.62 μmol·m^{-2}·s^{-1}. At WW stages, *A* of 'RS' had the highest value, 'GM' with 8.63 μmol·m^{-2}·s^{-1}, was in the middle, and 'BQ', with 6.93 μmol·m^{-2}·s^{-1}, was the lowest. The changes in C_i in response to water deficiency varied among the three cultivars. 'BQ' exhibited the greatest C_i (300.3 μmol·mol^{-1}) among the three cultivars at the WW stage. The lowest C_i of 'BQ' during drought was determined at D2, and C_i rose at D3. The highest C_i of 'RS' during drought conditions was 293.6 μmol·mol^{-1} at D3. g_s fell as the result of drought, and there was no significant difference among the three cultivars in the same water stress conditions. At WW stages, *E* of 'RS' was 2.82 mmol·m^{-2}·s^{-1}, which was significantly higher than that of 'BQ'. The WUE_i also demonstrated l differences in the WW stage, with 'GM' significantly higher than 'BQ'. The three cultivars' WUE_i tended to be highest at the D2 stage, despite the fact that 'GM' and 'RS'

doi:10.6342/NTU202400535

did not significantly differ between the drought stages. The photosystem II electron transport efficiency (ϕ_{PSII}) roughly declined with drought conditions in 'GM' and 'RS'. While ϕ_{PSII} did not show a significant decline in 'BQ'. At WW and D1, 'BQ' had the lowest ϕ_{PSII} compared with 'GM' and 'RS'. All three cultivars measured the increase in VPD with water deficiency and had the highest VPD at D3. At D2, VPD of 'GM' with 1.78 kPa was significantly lower than the other two cultivars.

3.2.2. *FvCB* variables of three grape cultivars under various drought conditions

The R_d of 'BQ' increased with drought. However, R_d of the hybrid cultivars remained consistent in the drought conditions (Table 3.7 and Fig. 3.8). At D3, g_m of the three cultivars showed a drop; prior to that, g_m did not show a significant decline. At the WW stage, g_m was 0.054 $mol \cdot m^{-2} \cdot s^{-1}$ in 'BQ' and 0.077 $mol \cdot m^{-2} \cdot s^{-1}$ in 'GM', which were much lower than 'RS'. g_m of the hybrid cultivars tended to slightly rise at the D2 stage, while that of 'RS' decreasing with increasing drought through all the stages. V_{cmax} of 'GM' and 'RS' decreased as the drought increased, while that of 'BQ' rose to 72.21 $\mu mol \cdot m^{-2} \cdot s^{-1}$ at D1 stage.

The results of light curves fitting were displayed in Table 3.7 and Fig. 3.8. As the drought stress increased, J_{max} and φ of the three cultivars reduced. While the hybrid cultivars and 'RS' responded differently to θ. In hybrid cultivars, θ decreased at D2, whereas 'RS' declined at D3.

3.2.3. The correlation of gas exchange variables and the FvCB variables under various drought conditions

According to the correlation matrix (Table 3.9), A, g_s, E, ϕ_{PSII}, g_m, J_{max} and φ had

doi:10.6342/NTU202400535

positive correlations with one another. The positive correlation of J_{max} to g_s and V_{cmax}, and WUE_i with g_m/g_s, were demonstrated as drought occurred. The negative correlation of C_i to WUE_i and g_m/g_s were observed at various drought conditions. The variations in R_d were observed at various drought stress, which negatively correlated to C_i, g_s, E, WUE_i and φ.

3.2.4. Contribution of the variables to the *A* difference under various medium water contents

Modeling results of numerical integrating the gas exchange variables revealed that A was mostly limited by RuBP (ribulose-1,5-bisphosphate) regeneration process, with the exception of that of 'BQ' at WW stage, which was limited by Rubisco carboxylation process. Compared to WW, A of 'BQ' and 'GM' declined by 72% and 74%, respectively, at D3 (Fig. 3.9). A of 'RS' at D3 decreased 90% of that at WW, which was the greatest drop of the three cultivars. In all three cultivars, g_{sc}, g_m and J_{max} were the main variables affecting the decrease in A at D2 and D3 (Fig. 3.9). With the grapevines suffering from drought, the contribution of g_{sc} and J_{max} on the reduction in A was increased. In 'GM' and 'RS', the negative effect of g_m on A reduced to 4.6% from D1 to D2. On the other hand, in 'BQ', g_m showed a 11% positive effect at D2. At D3, g_m reduced A in 'BQ' and 'RS' by 20%, and 'GM' by 26%. In all three cultivars at D2, biochemical factors were the main factor of the decline in A. In the extreme water deficient condition (D3), the hybrid cultivars demonstrated that the diffusional factors caused A to decrease by 40% and 45% in 'BQ' and 'GM', respectively, accounting for 50% to 60% of the overall contribution. While in 'RS', the A decrease was mainly caused by biochemical factors.

doi:10.6342/NTU202400535

3.2.5. Contribution of the variables to *A* response to various drought conditions of hybrid cultivars and vinifera grapes

The photosynthesis of 'RS' was used as the reference point to understand how different cultivars preformed in specific drought conditions (Fig. 3.10). *A* of 'BQ' and 'GM' were 37% and 18%, respectively, less efficient than 'RS' at the WW condition. The modeling results showed that the hybrid cultivars had roughly double the *A* of 'RS' at the extreme drought (D3). At WW and D1, the hybrid cultivar's g_m contributed 5% to 17% on its *A* being lower than 'RS'. At D3, g_m of the hybrid cultivars was the main factor that contributed to the greater *A* than 'RS'. At D2, θ contributed to 10% and 17% negative effect on *A* of 'BQ' and 'GM', respectively.

In 'BQ', biochemical and the diffusional factors had similar impact on the negative *A* to 'RS' at the WW condition (Fig. 3.10). The impact of biochemical factors increased at D1 and D2, with the J_{max} and θ accounting for the majority of the effect. In 'GM', diffusional factors, particularly g_m, were the primary cause of the less efficient *A* at WW and D1. At D3, 'BQ' had *A* 70% greater than 'RS', with biochemical and diffusional factors accounting for 27.5% and 42.5%, respectively, of the difference. Regarding to 'GM', the two groups had an equal impact on its higher *A* than 'RS'.

3.3. Trichome density and stomata density of the hybrid and vinifera grapes

The hybrid cultivars 'BQ' and 'GM' both had trichome on the abaxial side, while 'RS' was glossy (Fig. 3.11). Trichomes were found in significantly different numbers on the leaf back of the hybrid cultivars 'BQ' and 'GM', with 71 and 259 cm^{-2}, respectively (Table 3.10). There were none or 1 trichome on the leaf back of 'RS' (Fig. 3.11). The stomata were observed by the optical microscope with cleaning technique showed in

doi:10.6342/NTU202400535

Fig. 3.12. The stomata density of the three cultivars ranged from 121 to 132 μm^{-2} in each observation (Table 3.10), which did not show a significand difference between them.

3.3.1 Relationship of trichome densities and gas exchange variables

A scatter graph of the gas exchange variables in relation to the trichome densities is shown in Fig. 3.13. VPD and WUE_i were highly correlated with trichome densities with correlation coefficients (r) of 0.942 and 0.975, respectively. A and g_s tended to negatively correlated with trichome densities.

doi:10.6342/NTU202400535

Table 3.1. Gas exchange variables of well-watered ‘Black Queen’, ‘Golden Muscat’ and ‘Riesling’ grape leaves. Photosynthesis assimilation rate (A), intercellular CO_2 concentration (C_i), stomatal conductance (g_s), transpiration rate (E), intrinsic water use efficiency (WUE_i, A/g_s,), photosystem II (PSII) electron transport efficiency (ϕ_{PSII}), and leaf vapor pressure deficit (VPD) were measured at ambient CO_2 concentration (C_a, 400 μmol·mol^{-1}) and saturating photosynthetic light intensity of 1200 μmol·m^{-2}·s^{-1}.

Cultivars	A (μmolCO_2·m^{-2}·s^{-1})	C_i (μmol·mol^{-1})	g_s (mol H_2O·m^{-2}·s^{-2})	E (mmol·m^{-2}·s^{-1})	WUE_i (μmol CO_2·mol H_2O^{-1})	ϕ_{PSII}	VPD (kPa)
Black Queen	7.48± 1.07 b[x]	307.58± 10.68 a	0.161± 0.002 b	3.05± 0.08 b	46.78± 6.29 b	0.099±0.009 B	1.90±0.02b
Golden Muscat	7.39± 0.28 b	272.93± 12.31 b	0.110± 0.008 c	2.24± 0.16 c	68.65± 7.73 a	0.113±0.010 B	2.04±0.07a
Riesling	11.59± 0.64 a	307.10± 4.29 a	0.260± 0.014 a	4.37± 0.24 a	45.58± 2.47 b	0.160±0.007 A	1.71±0.01c

[x] Data represented mean ± standard error (n = 3). Lower case letters indicate significant difference between cultivars by LSD test ($P < 0.05$).

doi:10.6342/NTU202400535

Table 3.2. *FvCB* variables of well-watered 'Black Queen', 'Golden Muscat' and 'Riesling' grape leaves. Day respiration rates (R_d) were obtained by Yin's method (Yin et al., 2011). Mesophyll conductance (g_m) and maximum rate of Rubisco carboxylation (V_{cmax}) were generated using the approach published by Moualeu-Ngangue *et al*., 2017. Maximum electron transport capacity at saturating light (J_{max}) and initial slope of electron transport rate versus light (φ) were generated using the model by Sharkey *et al*., 2016.

Cultivars	R_d (μmol CO_2 ·$m^{-2}s^{-1}$)	g_m (mol CO_2·$m^{-2}s^{-1}$)	V_{cmax} (μmol·m^{-2}·s^{-1})	J_{max} (μmol·m^{-2}·s^{-1})	φ	θ
Black Queen	0.974±0.203 a[x]	0.064±0.021 a	58.07±8.46 ab	53.40±4.87 b	0.238±0.013 a	0.902±0.066 a
Golden Muscat	0.945±0.248 a	0.064±0.007 a	56.21±3.86 b	64.30±6.01 b	0.273±0.018 a	0.819±0.048 a
Riesling	0.962±0.048 a	0.088±0.020 a	80.64±7.30 a	99.58±15.13 a	0.288±0.019 a	0.708±0.085 a

[x] Data represented mean ± standard error (n = 3). Lower case letters indicate significant difference between cultivars by LSD test ($P < 0.05$).

doi:10.6342/NTU202400535

Table 3.3. The correlation matrix of leaf gas exchange and *FvCB* variables of the tree tested grapevine cultivars at well-watered condition. Data represent the Pearson correlation between the two variables, and the dark blue represent the higher liner correlation. The correlation was counted by every repeat of the three cultivars.

	A	C_i	g_s	E	WUE_i	ϕ_{PSII}	VPD	R_d	g_m	V_{cmax}	J_{max}	φ	θ	g_m/g_s
A	1.000													
C_i	0.105	1.000												
g_s	0.828*	0.617	1.000											
E	0.820*	0.630	0.994*	1.000										
WUE_i	-0.169	-0.998*	-0.664*	-0.677*	1.000									
ϕ_{PSII}	0.888*	-0.033	0.694*	0.652*	-0.019	1.000								
VPD	-0.679*	-0.679*	-0.901*	-0.862*	0.712*	-0.634	1.000							
R_d	-0.191	0.517	0.099	0.122	-0.503	-0.180	-0.123	1.000						
g_m	0.776*	-0.236	0.427	0.463	0.176	0.515	-0.191	-0.326	1.000					
V_{cmax}	0.497	0.372	0.631*	0.588	-0.392	0.745*	-0.671*	0.216	-0.058	1.000				
J_{max}	0.703*	0.169	0.603*	0.571	-0.207	0.819*	-0.601	0.178	0.270	0.725*	1.000			
φ	0.559	-0.232	0.248	0.257	0.193	0.555*	-0.080	-0.017	0.478	0.226	0.767*	1.000		
θ	-0.682*	0.080	-0.533	-0.498	-0.043	-0.769*	0.410	0.160	-0.287	-0.503	-0.744*	-0.639*	1.000	
g_m/g_s	-0.026	-0.920*	-0.538	-0.513	0.909*	-0.055	0.697*	-0.519	0.471	-0.540	-0.282	0.220	0.024	1.000

* represents the Pearson correlation of the two variables by t-test ($P < 0.05$) with degrees of freedom = 9-2.

doi:10.6342/NTU202400535

Table 3.4. The media water contents of the three cultivars during the experiment.

Cultivar	Condition	medium water content (%)	
Black Queen	WW	198±23	a A[x]
	D1	64±2	a A
	D2	40±1	b A
	D3	26±2	c A
Golden Muscat	WW	258±11	a A
	D1	47±3	b A
	D2	35±2	b A
	D3	25±2	c A
Riesling	WW	198±9	a A
	D1	54±11	b A
	D2	37±8	b A
	D3	27±6	b A

[x] Data represented mean ± standard error (n = 3).. Lower case indicated significant difference of the treatment in the cultivar, and capital case indicated significant difference of same treatment between the cultivars by LSD test ($P < 0.05$).

doi:10.6342/NTU202400535

Table 3.5. Gas exchange variables of 'Black Queen' (BQ), 'Golden Muscat' (GM) and 'Riesling' (RS) vines, well-watered (WW), or subjected to mild (D1), moderate (D2), or extreme (D3) drought condition. Photosynthesis assimilation rate (A), intercellular CO_2 concentration (C_i), stomatal conductance (g_s), transpiration rate (E), and water use efficiency (WUE_i, A/g_s,) were measured at ambient CO_2 concentration (C_a, 400 μmol·mol^{-1}) and a saturating photosynthetic light intensity of 1200 μmol·m^{-2}·s^{-1}.

Cultivar	Condition	A ($\mu molCO_2 \cdot m^{-2} \cdot s^{-1}$)	C_i ($\mu mol \cdot mol^{-1}$)	g_s ($molH_2O \cdot m^{-2} \cdot s^{-2}$)	E ($mmol \cdot m^{-2} \cdot s^{-1}$)	WUE_i ($\mu molCO_2 \cdot molH_2O^{-1}$)	ϕ_{PSII}	VPD (kPa)
BQ	WW	6.93±0.23 a B[x]	300.3±9.1 a A	0.136±0.011 a A	2.35±0.09 a AB	52.46±5.41 c B	0.073±0.008 ab B	1.74±0.06 b A
	D1	6.82±0.76 a A	301.9±9.8 a A	0.136±0.017 a A	2.33±0.21 a A	51.55±5.92 c A	0.080±0.005 a B	1.72±0.06 b A
	D2	5.88±0.55 a A	256.2±11.7 b A	0.075±0.013 b A	1.46±0.22 b A	81.11±7.52 a A	0.076±0.006 ab A	1.94±0.04 a A
	D3	1.90±0.59 b A	281.3±17.4 ab A	0.027±0.005 c A	0.54±0.11 c A	66.49±10.86 b A	0.056±0.005 b A	1.97±0.03 a A
GM	WW	8.63±0.93 a AB	275.3±6.2 a B	0.129±0.011 a A	2.08±0.16 a B	67.87±3.76 a A	0.116±0.012 a A	1.62±0.02 b A
	D1	7.70±0.27 ab A	281.1±8.6 a A	0.121±0.005 a A	2.05±0.12 a A	64.38±5.03 a A	0.114±0.005 a AB	1.70±0.06 b A
	D2	6.58±0.33 b A	255.4±13.5 a A	0.084±0.014 b A	1.49±0.22 b A	81.28±8.94 a A	0.099±0.009 ab A	1.78±0.05 ab B
	D3	2.57±0.46 c A	256.9±12.9 a A	0.031±0.003 c A	0.60±0.03 c A	81.87±8.37 a A	0.075±0.007 bc A	1.95±0.08 a A
RS	WW	10.66±0.66 a A	278.8±5.3 b AB	0.164±0.010 a A	2.82±0.14 a A	66.09±2.97 a AB	0.139±0.010 a A	1.73±0.04 b A
	D1	8.97±1.33 ab A	280.9±13.3 b A	0.148±0.033 ab A	2.48±0.50 a A	69.59±12.09 a A	0.122±0.016 ab A	1.71±0.05 b A
	D2	6.16±0.86 b A	263.4±22.8 b A	0.083±0.011 bc A	1.54±0.20 ab A	76.70±14.17 a A	0.084±0.013 b A	1.84±0.03 b A
	D3	1.62±0.34 c A	293.6±2.3 a A	0.026±0.006 c A	0.52±0.10 bc A	56.44±1.26 a A	0.069±0.021 b A	1.98±0.02 a A

[x] Data represented mean ± standard error (n = 3). Lower case indicated significant difference of the treatment in the cultivar, and capital case indicated significant difference of same treatment between the cultivars by LSD test ($P < 0.05$).

doi:10.6342/NTU202400535

Table 3.6. Pooled data of the gas exchange variables in Table 3.5.

	A ($\mu molCO_2 \cdot m^{-2} \cdot s^{-1}$)	C_i ($\mu mol \cdot mol^{-1}$)	g_s ($molH_2O \cdot m^{-2} \cdot s^{-2}$)	E ($mmol \cdot m^{-2} \cdot s^{-1}$)	WUE_i ($\mu molCO_2 \cdot molH_2O^{-1}$)	ϕ_{PSII}	VPD (kPa)
Cultivars							
Black Queen	5.36±0.67 b	286.1±7.6a	0.094±0.015 a	1.67±0.23 ab	62.13±4.87 a	0.072±0.004 b	1.85±0.04 a
Golden Muscat	6.37±0.74 ab	267.2±5.7b	0.091±0.012 a	1.56±0.19 b	73.80±3.77 a	0.101±0.006 a	1.77±0.04 b
Riesling	7.20±1.09 a	277.2±7.3ab	0.110±0.018 a	1.92±0.05 a	69.01±4.95 a	0.107±0.010 a	1.80±0.03 ab
Condition							
WW	8.74±0.64 a	284.8±5.3a	0.143±0.007 a	2.42±0.13 a	62.01±3.19 b	0.109±0.011 a	1.70±0.03 c
D1	7.73±0.52 a	286.9±6.6a	0.132±0.011 a	2.24±0.17 a	62.85±5.16 b	0.104±0.008 ab	1.72±0.03 c
D2	6.18±0.33 b	257.9±8.4b	0.0810.007 b	1.49±0.11 b	79.70±5.35 a	0.087±0.006 b	1.85±0.03 b
D3	2.02±0.30 c	277.9±9.5ab	0.029±0.002 c	0.57±0.04 c	68.58±6.21 ab	0.067±0.006 c	1.97±0.03 a
Cultivar	*[y]	0.49	n.s.	n.s.	24.3	***	n.s.
Condition	***	*	***	***	n.s.	***	***
Cultivar x condition	n.s.	n.s.	n.s.	n.s.	n.s.	n.s.	n.s.

[x] Data represented mean ± standard error. Lower case indicated significant difference of the treatment in the cultivar, and capital case indicated significant difference of same treatment between the cultivars by LSD test ($P < 0.05$).

[y] '*', '**', '***' indicate significant at $P < 0.05,0.01,0.001$; n.s. non-significant.

doi:10.6342/NTU202400535

Table 3.7. *FvCB* modeling of 'Black Queen' (BQ), 'Golden Muscat' (GM) and 'Riesling' (RS) grapevines, well-watered (WW), or subjected to mild (D1), moderate (D2), or extreme (D3) drought condition. Day respiration rates (R_d) obtain by Yin's method (Yin et al., 2011). Mesophyll conductance (g_m) and maximum rate of Rubisco carboxylation (V_{cmax}) were generated using the approach published by Moualeu-Ngangue *et al*., 2017. Maximum electron transport capacity at saturating light (J_{max}) and initial slope of electron transport rate versus light (φ) were generated using the model by Sharkey *et al*., 2016.

Cultivar	Condition	R_d ($\mu molCO_2 \cdot m^{-2}s^{-1}$)	g_m ($molCO_2 \cdot m^{-2}s^{-1}$)	V_{cmax} ($\mu mol \cdot m^{-2} \cdot s^{-1}$)	J_{max} ($\mu mol \cdot m^{-2} \cdot s^{-1}$)	φ	θ
BQ	WW	0.647±0.047 c A[x]	0.054±0.017 ab B	39.09±3.22 b B	62.22±7.53 a A	0.275±0.008 a A	0.726±0.050 a A
	D1	0.702±0.162 bc A	0.069±0.011 ab A	72.21±4.45 a A	52.74±6.98 ab A	0.239±0.027 ab A	0.840±0.047 a A
	D2	0.982±0.060 b B	0.096±0.022 a A	45.57±3.43 b B	45.15±8.62 ab A	0.179±0.032 b AB	0.472±0.085 b A
	D3	1.399±0.082 a A	0.017±0.013 b A	45.32±9.41 b A	25.75±3.41 b A	0.092±0.001 c A	0.747±0.149 ab A
GM	WW	1.010±0.155 a A	0.077±0.014 a B	72.89±5.81 ab A	75.77±10.60a A	0.306±0.025 ab A	0.807±0.077 a A
	D1	1.077±0.103 a A	0.055±0.005 a A	94.02±8.30 a A	70.52±15.90a A	0.221±0.023 bc A	0.939±0.013 a A
	D2	1.298±0.047 a A	0.058±0.007 a A	69.05±15.68 ab AB	55.38±9.26 ab A	0.201±0.012 c A	0.051±0.276 a A
	D3	1.097±0.242 a A	0.014±0.002 b A	49.00±8.48 b A	33.51±7.39 b A	0.140±0.049 c A	0.530±0.279 a A
RS	WW	1.009±0.163 a A	0.141±0.013 a A	64.64±4.08 a A	84.13±3.81 a A	0.287±0.016 a A	0.724±0.114 a A
	D1	1.141±0.288 a A	0.096±0.024 a A	76.57±7.16 a A	86.68±19.18a A	0.214±0.040 a A	0.837±0.022 a A
	D2	1.451±0.082 a A	0.022±0.017 a A	67.73±3.30 a A	51.42±6.24 ab A	0.117±0.002 b B	0.927±0.025 a A
	D3	1.231±0.029 a A	0.007±0.001 b A	46.50±12.23 b A	22.25±0.89 b A	0.047±0.047 b A	0.389±0.171 b A
Cultivar		n.s.[y]	*	**	n.s.	n.s.	n.s.
Condition		*	***	***	***	***	n.s.
Cultivar x Condition		n.s.	*	n.s.	n.s.	n.s.	n.s.

[x] Data represented mean ± standard error (n = 3). Lower case indicated significant difference of the treatment in the cultivar, and capital case indicated significant difference of same treatment between the cultivars by LSD test ($P < 0.05$).

doi:10.6342/NTU202400535

Table 3.8. Pooled data of FVCB variables in Table 3.7.

	R_d ($\mu molCO_2 \cdot m^{-2}s^{-1}$)	g_m ($molCO_2 \cdot m^{-2}s^{-1}$)	V_{cmax} ($\mu mol \cdot m^{-2} \cdot s^{-1}$)	J_{max} ($\mu mol \cdot m^{-2} \cdot s^{-1}$)	φ	θ
Cultivars						
Black Queen	0.890±0.097 b	0.064±0.011 b	51.02±4.63 c	48.34±5.04 b	0.206±0.023 a	0.692±0.055 a
Golden Muscat	1.121±0.073 a	0.052±0.008 b	71.24±6.50 ab	58.76±6.90 ab	0.217±0.022 a	0.696±0.102 a
Riesling	1.206±0.096 a	0.093±0.016 a	65.44±4.14 b	64.66±9.17 a	0.047±0.030 a	0.749±0.069 a
Condition						
WW	0.889±0.090 c	0.092±0.015 a	58.87±5.58 a	74.04±5.05 a	0.289±0.010 a	0.753±0.044 ab
D1	0.974±0.121 bc	0.076±0.010 a	80.93±4.77 b	69.98±8.94 a	0.224±0.016 b	0.872±0.023 a
D2	1.244±0.076 a	0.081±0.011 a	60.78±6.07 a	50.67±4.34 b	0.166±0.016 c	0.636±0.111 b
D3	1.222±0.107 a	0.015±0.004 b	47.23±4.69 a	28.05±3.52 c	0.100±0.027 d	0.552±0.129 b
Cultivar	n.s.[y]	*	**	n.s.	n.s.	n.s.
Condition	*	***	***	***	***	n.s.
Cultivar x condition	n.s.	*	n.s.	n.s.	n.s.	n.s.

[x] Data represented mean ± standard error (n = 3). Lower case indicated significant difference of the treatment in the cultivar, and capital case indicated significant difference of same treatment between the cultivars by LSD test ($P < 0.05$).

[y] '*', '**', '***' indicate significant at $P < 0.05,0.01,0.001$; n.s. non-significant.

doi:10.6342/NTU202400535

Table 3.9. The correlation matrix of leaf gas exchange and *FvCB* variables under various drought conditions. Data represent the Pearson correlation between two variables. Dark blue represents the higher liner correlation. The correlations were counted by the mean of the data of three cultivars under the various media water content.

	A	C_i	g_s	E	WUE_i	ϕ_{PSII}	VPD	R_d	g_m	V_{cmax}	J_{max}	φ	θ	g_m/g_s
A	1.000													
C_i	0.059	1.000												
g_s	0.951*	0.337	1.000											
E	0.951*	0.317	0.997*	1.000										
WUE_i	-0.066	-0.990*	-0.334	-0.315	1.000									
ϕ_{PSII}	0.866*	-0.086	0.751*	0.733*	0.087	1.000								
VPD	-0.871*	-0.279	-0.900*	-0.870*	0.292	-0.742*	1.000							
R_d	-0.376	-0.528	-0.566*	-0.568*	0.551	-0.081	0.441	1.000						
g_m	0.843*	-0.171	0.729*	0.761*	0.174	0.700*	-0.495	-0.159	1.000					
V_{cmax}	0.475	0.143	0.464	0.426	-0.166	0.529	-0.688*	-0.084	0.104	1.000				
J_{max}	0.960*	0.102	0.927*	0.913*	-0.091	0.897*	-0.900*	-0.332	0.714*	0.568*	1.000			
φ	0.863*	0.179	0.884*	0.870*	-0.206	0.666*	-0.874*	-0.670*	0.580*	0.440	0.833*	1.000		
θ	0.350	0.414	0.453	0.441	-0.382	0.225	-0.416	-0.185	0.240	0.479	0.431	0.276	1.000	
g_m/g_s	0.249	-0.651*	0.049	0.102	0.664*	0.134	0.169	0.243	0.666*	-0.265	0.105	-0.018	-0.050	1.000

* represents the Pearson correlation of the two variables by t-test ($P < 0.05$) with degrees of freedom = 12-2.

doi:10.6342/NTU202400535

Table 3.10. Trichome and stomata numbers of the three grape cultivars. Trichomes were observed under the dissecting microscope with 30X magnification. Stomata were observed under the optical microscope with 100X magnification.

Cultivars	Trichome (number cm^{-2})	Stomata (number μm^{-2})
Black Queen	71±17 b[x]	121±6 a
Golden Muscat	259±19 a	128±6 a
Riesling	0±0 c	132±10 a

[x] Data represented mean ± standard error (n = 3). Lower case letters indicate significant difference between cultivars by LSD test ($P < 0.05$).

doi:10.6342/NTU202400535

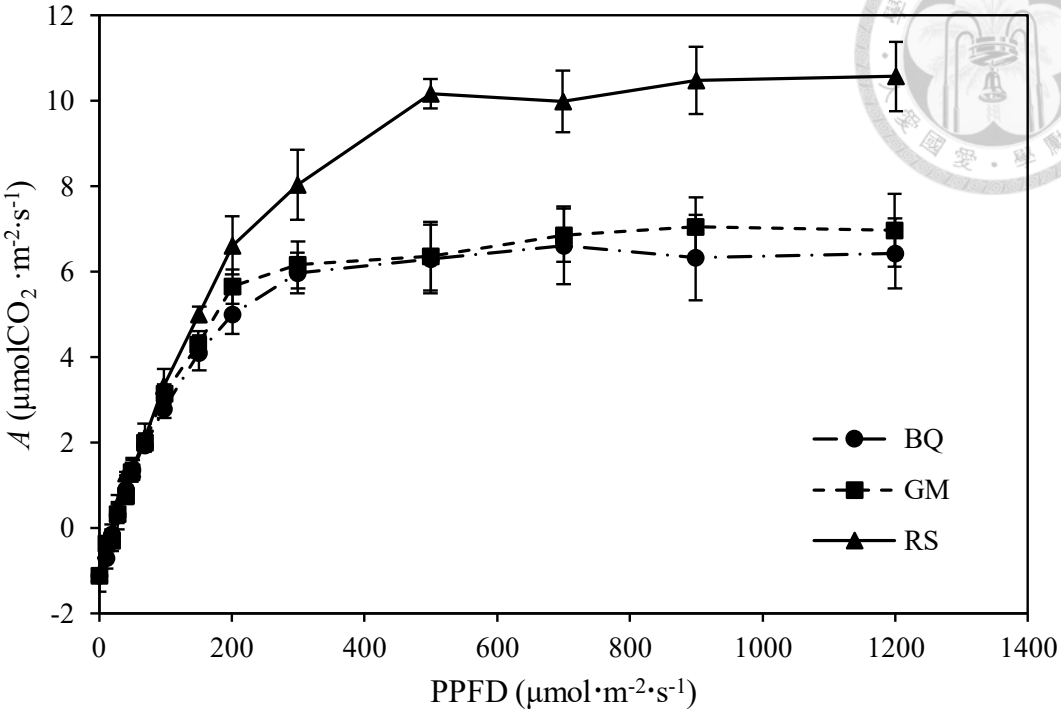

Fig. 3.1. Net assimilation rates (*A*) of 'Black Queen' (BQ), 'Golden Muscat' (GM) and 'Riesling' (RS) grape leaves against photosynthetic photon flux density (PPFD) at 25℃, 400 μmol·mol^{-1} CO_2 and optimal water status. Each data show as mean with stander error (n=3).

doi:10.6342/NTU202400535

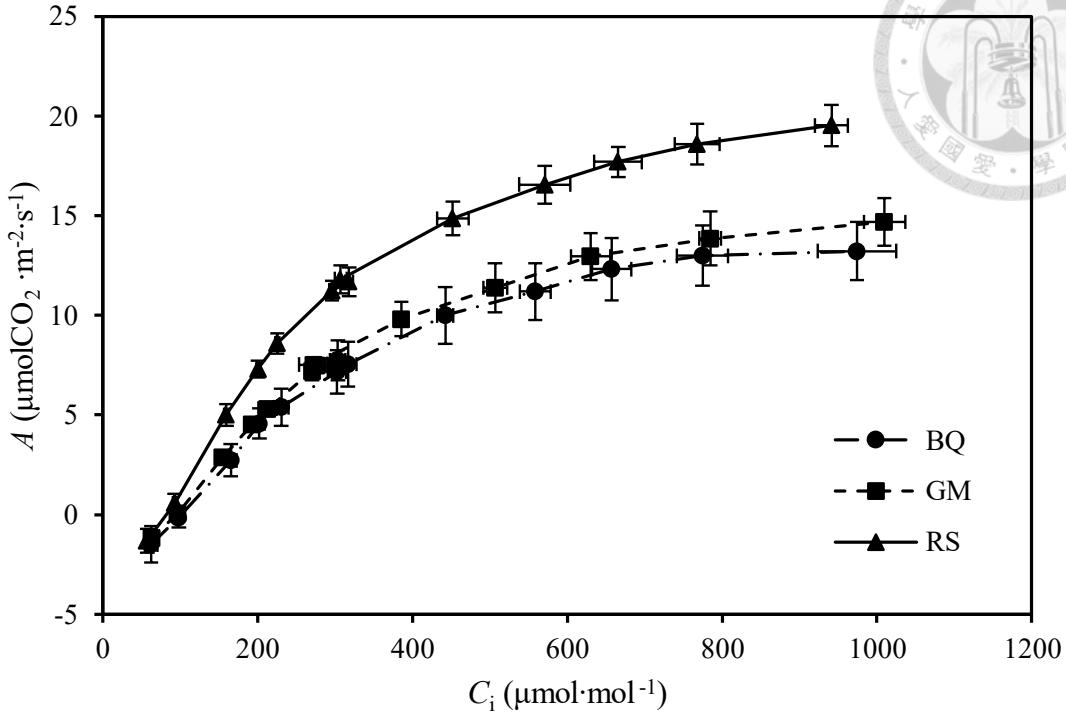

Fig. 3.2. CO_2 response curve (A-C_i curve) of 'Black Queen' (BQ), 'Golden Muscat' (GM) and 'Riesling' (RS) leaves at 25℃, light intensity 1200 μmol·m^{-2}·s^{-1} and optimal water status. Each data show as mean with stander error (n=3).

doi:10.6342/NTU202400535

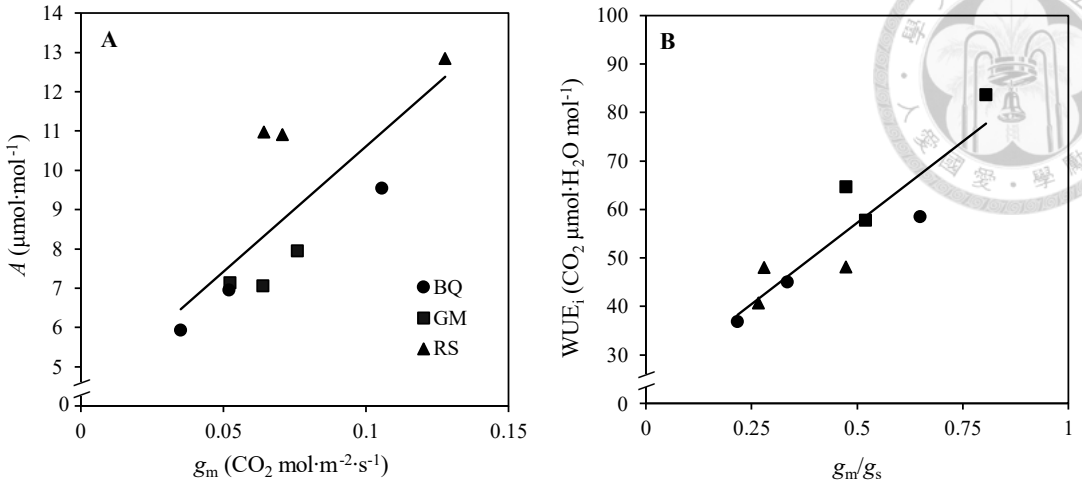

Fig. 3.3. Functions of (**A**) photosynthetic assimilation rate (*A*) against mesophyll conductance (g_m) and (**B**) intrinsic water use efficiency (WUE_i) against ratio of g_m to stomatal conductance (g_s) in 'Black Queen' ('BQ'), 'Golden Muscat' ('GM') and 'Riesling' ('RS') grape leaves. Gas exchange measurements were taken in well-watered condition. Each data show as mean with stander error (n=3). $A = 63.884g_m + 4.2275$, r=0.776. $WUE_i=67.126g_m/g_s + 23.697$, r = 0.909.

doi:10.6342/NTU202400535

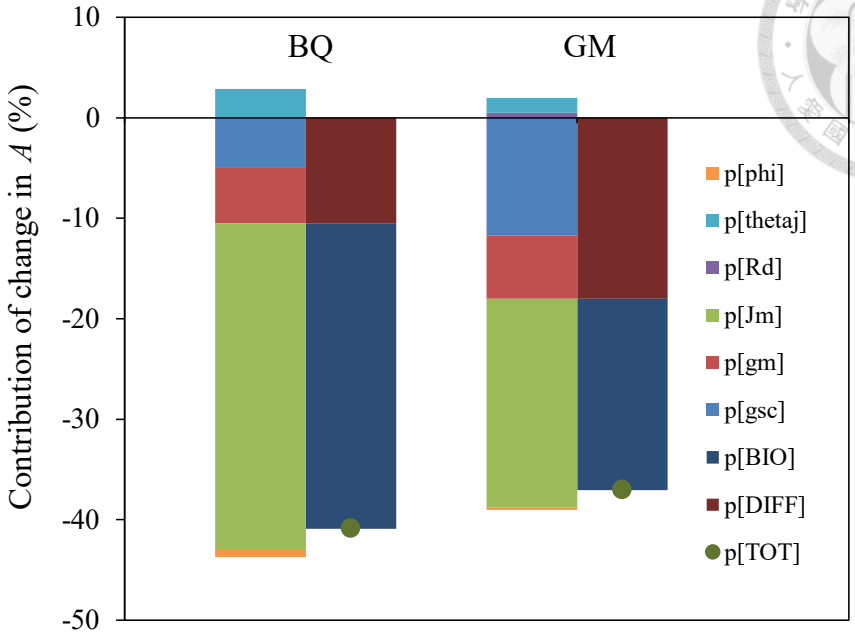

Fig. 3.4. The contribution of gas exchange variables of 'Black Queen' (BQ) and 'Golden Muscat' (GM) to the difference in *A* between these two hybrids and the vinifera 'Riesling' at well-watered condition. Leaf gas exchange of well-watered vines was measured at 25℃, light intensity 1200 μmol·m^{-2}·s^{-1}. The net assimilation rates for 'Riesling' were used as the reference. The left bar of each cultivar shows partition change of individual variables, p[*x*] indicate the contribution of variable *x* to *A*. p[phi]=initial slope of electron transport rate versus light, φ; p[thetaj]=convexity factor of electron transport rate versus light; p[Rd]=day respiration rate, R_d; [Jm]= maximum electron transport capacity at saturating light J_{max}; p[gm]=mesophyll conductance, g_m; p[gsc]=CO_2 stomatal conductance, g_{sc}. The right bar of each cultivar shows total change of *A* (p[TOT]), contribution of biochemical factors (p[BIO]=p[phi]+ p[thetaj]+p[Rd]+p[Jm]) and diffusional factors (p[DIFF]=p[gm]+p[gsc]).

doi:10.6342/NTU202400535

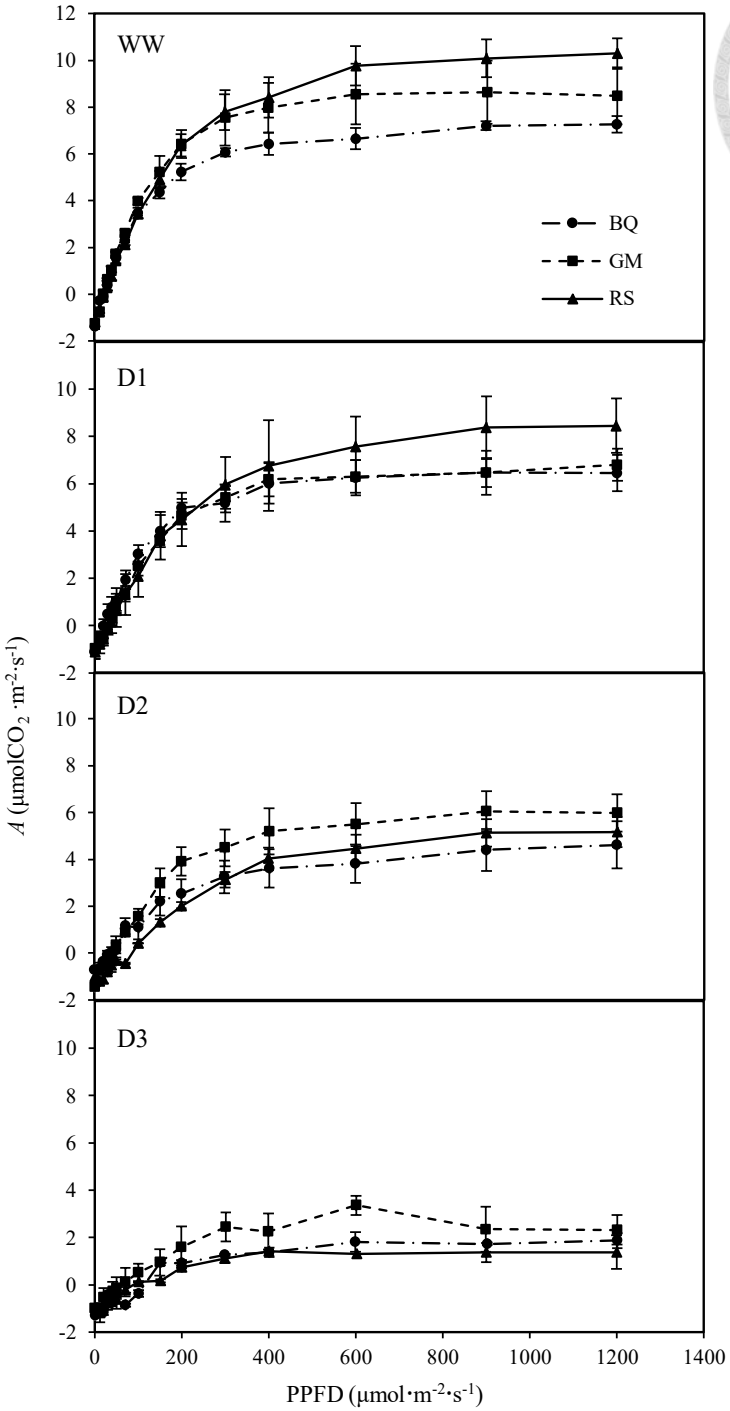

Fig. 3.5. Net assimilation rates (*A*) of 'Black Queen' (BQ), 'Golden Muscat' (GM) and 'Riesling' (RS) leaves against photosynthetic photon flux density (PPFD) at 25℃, 400 μmol·mol^{-1} CO_2 under various drought conditions. WW, well-watered condition; D1, slight stress; D2, moderate stressed; D3, extreme stress. Each data show as mean with stander error (n=3).

doi:10.6342/NTU202400535

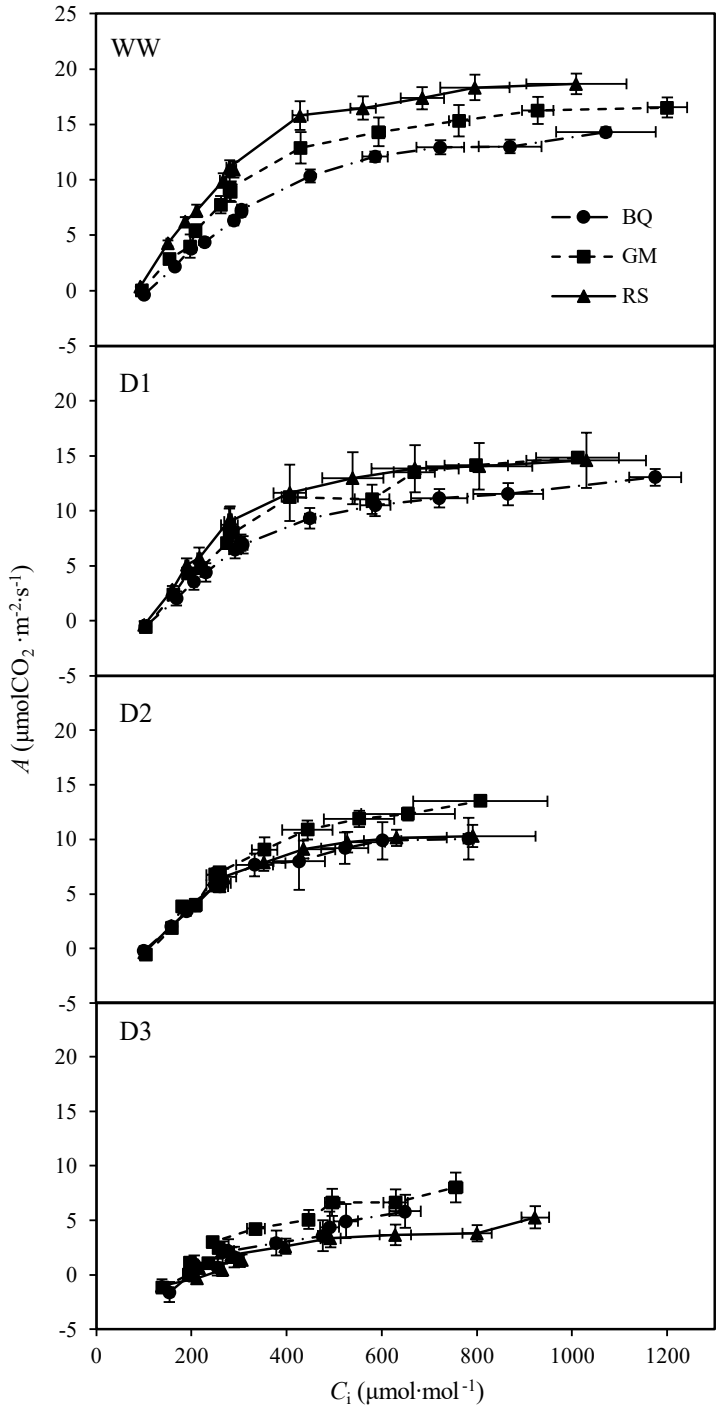

Fig. 3.6. CO_2 response curve (A-C_i curve) of 'Black Queen' (BQ), 'Golden Muscat' (GM) and 'Riesling' (RS) leaves at 25℃, light intensity 1200 μmol·m^{-2}·s^{-1} under under various drought conditions. WW, well-watered condition; D1, slight stress; D2, moderate stressed; D3, extreme stress. Each data show as mean with stander error (n=3).

doi:10.6342/NTU202400535

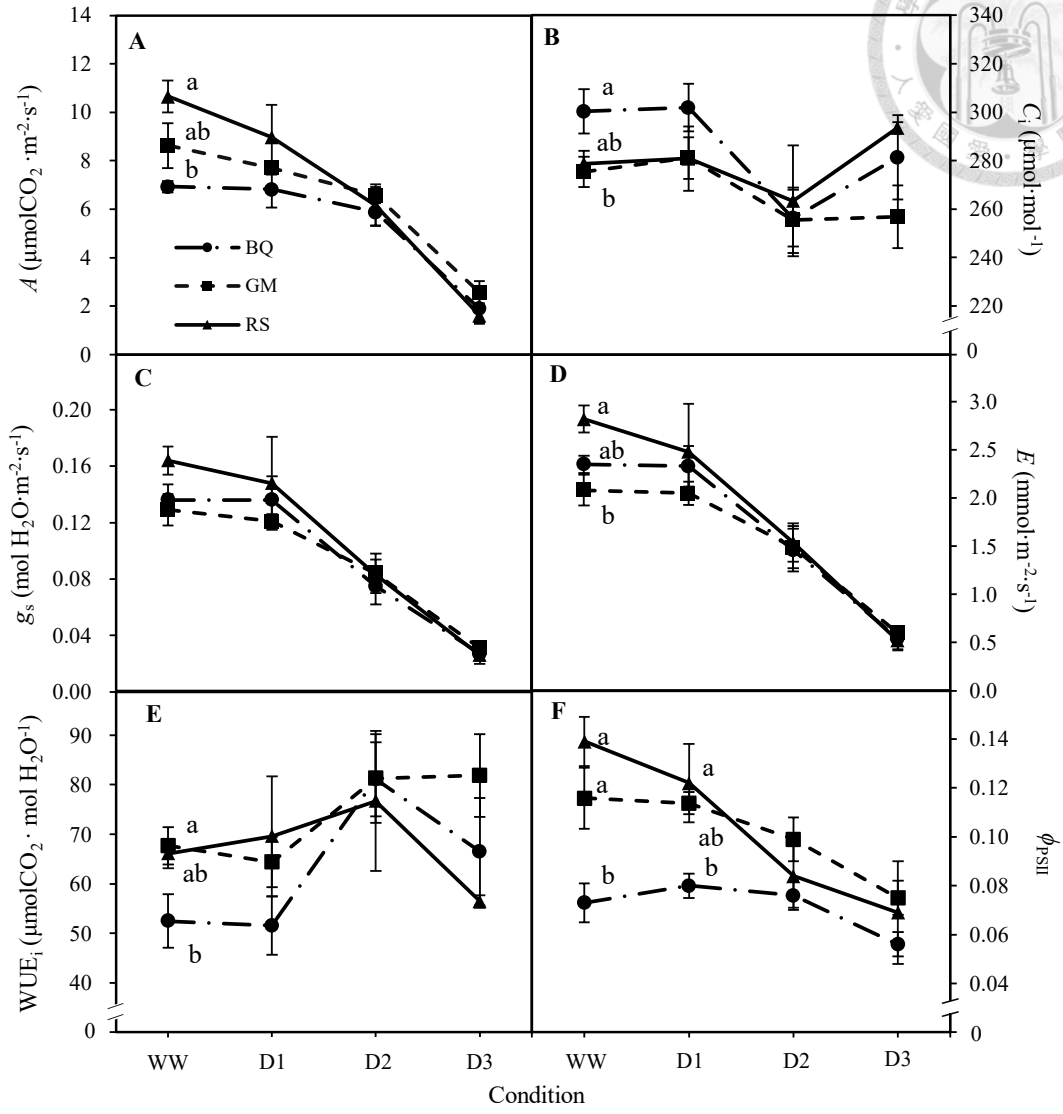

Fig 3.7. Gas exchange variables of Black Queen' (BQ), 'Golden Muscat' (GM) and 'Riesling' (RS) at ambient CO_2 concentration (C_a, 400 μmol·mol^{-1}) saturating light 1200 μmol·m^{-2}·s^{-1} and 25℃ under various drought conditions. **A:** Photosynthesis assimilation rate (A); **B:** intercellular CO_2 concentration (C_i); **C:** stomatal conductance (g_s); **D:** transpiration rate (E); **E:** intrinsic water use efficiency (WUE$_i$, A/g_s,); **F:** photosystem II (PSII) electron transport efficiency (ϕ_{PSII}). WW: well-watered condition; D1: slight stress; D2: moderate stressed; D3: extreme stress. Data from table 3.5. Each data show as mean with stander error (n=3). Lower case letters indicate significant difference between cultivars by LSD test (P<0.05) in the same water condition.

doi:10.6342/NTU202400535

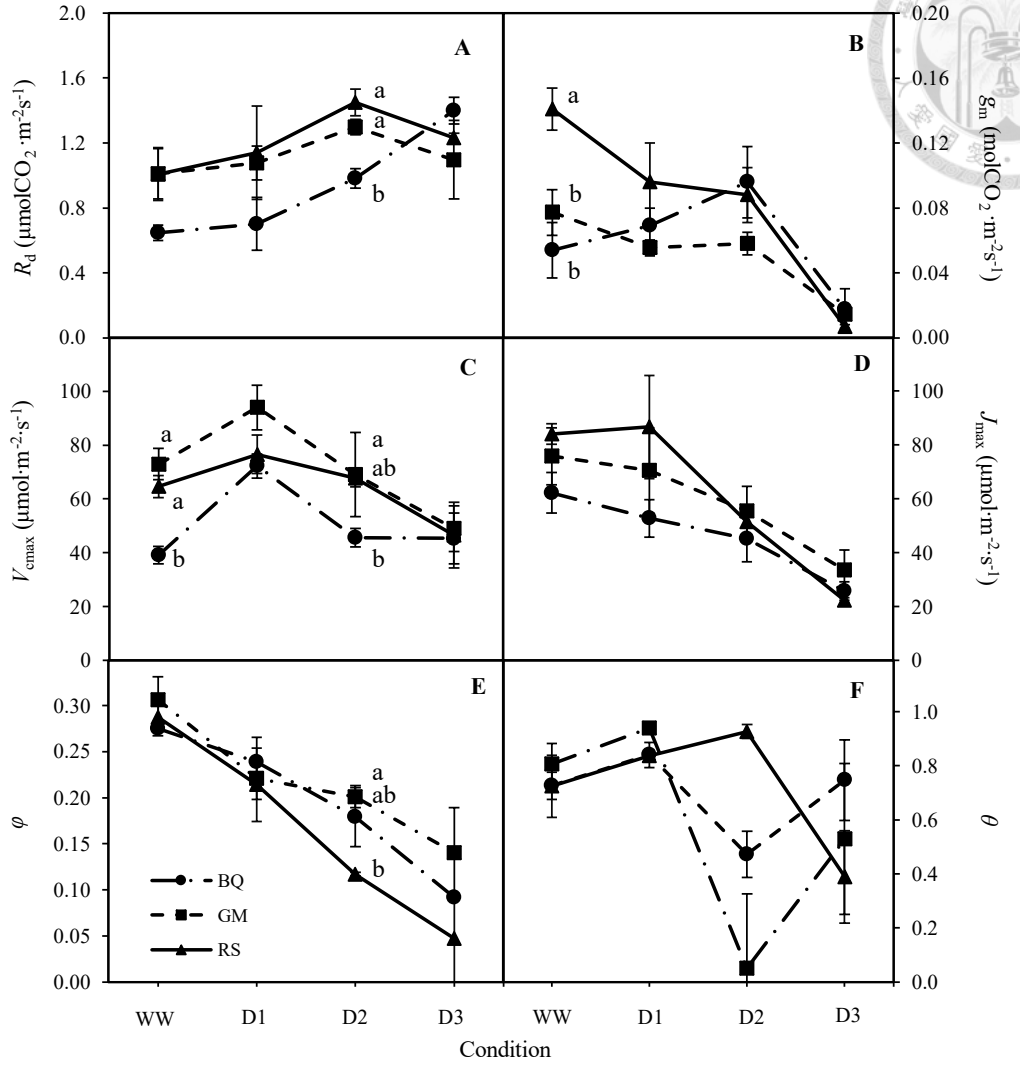

Fig. 3.8. *FvCB* variables of Black Queen' (BQ), 'Golden Muscat' (GM) and 'Riesling' (RS) under various drought conditions. **A:** Day respiration rates (R_d) obtain by Yin method (Yin et al., 2011). **B:** mesophyll conductance (g_m) and **C:** maximum rate of Rubisco carboxylation (V_{cmax})generated by Moualeu-Ngangue *et al*. (2017). **D:** maximum electron transport capacity at saturating light (J_{max}), **E.** initial slope of electron transport rate versus light (φ) and **F:** convexity factor of electron transport rate versus light (θ) obtain by Sharkey *et al*. (2016). WW, well-watered condition; D1, slight stress; D2, moderate stressed; D3, extreme stress. Data from table 3.7. Each data show as mean with stander error (n=3). Lower case letters indicate significant difference between cultivars by LSD test (P<0.05) in the same water condition.

doi:10.6342/NTU202400535

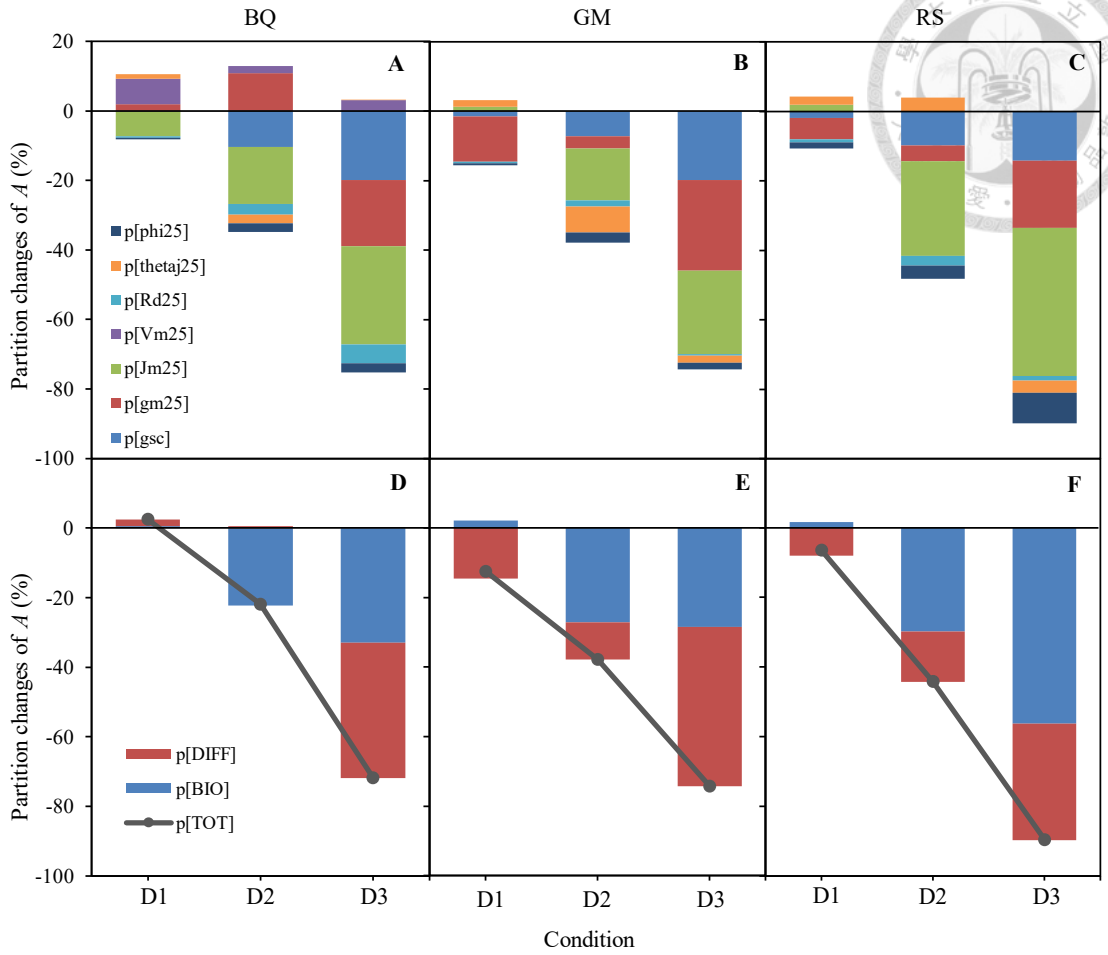

Fig. 3.9. The contribution of gas exchange variables to the changes of *A* in 'Black Queen' (BQ), 'Golden Muscat' (GM) and 'Riesling' (RS) under various drought conditions. Leaf gas exchange of vines was measured at 25℃, light intensity 1200 μmol·m^{-2}·s^{-1}. **A-C** p[*x*] indicate the contribution of variable *x* to *A*. p[phi]=initial slope of electron transport rate versus light (φ); p[thetaj]=convexity factor of electron transport rate versus light (θ); p[Rd]=day respiration rate (R_d); p[Jm]=maximum electron transport capacity at saturating light (J_{max}); p[gm]=mesophyll conductance (g_m); p[gsc]=CO_2 stomatal conductance (g_{sc}). **D-F** shows total change of *A* (p[TOT]), contribution of biochemical factors (p[BIO]=p[phi]+ p[thetaj]+p[Rd]+p[Jm]) and diffusional factors (p[DIFF]=p[gm]+p[gsc]). WW, well-watered condition; D1, slight stress; D2, moderate stressed; D3, extreme stress.

doi:10.6342/NTU202400535

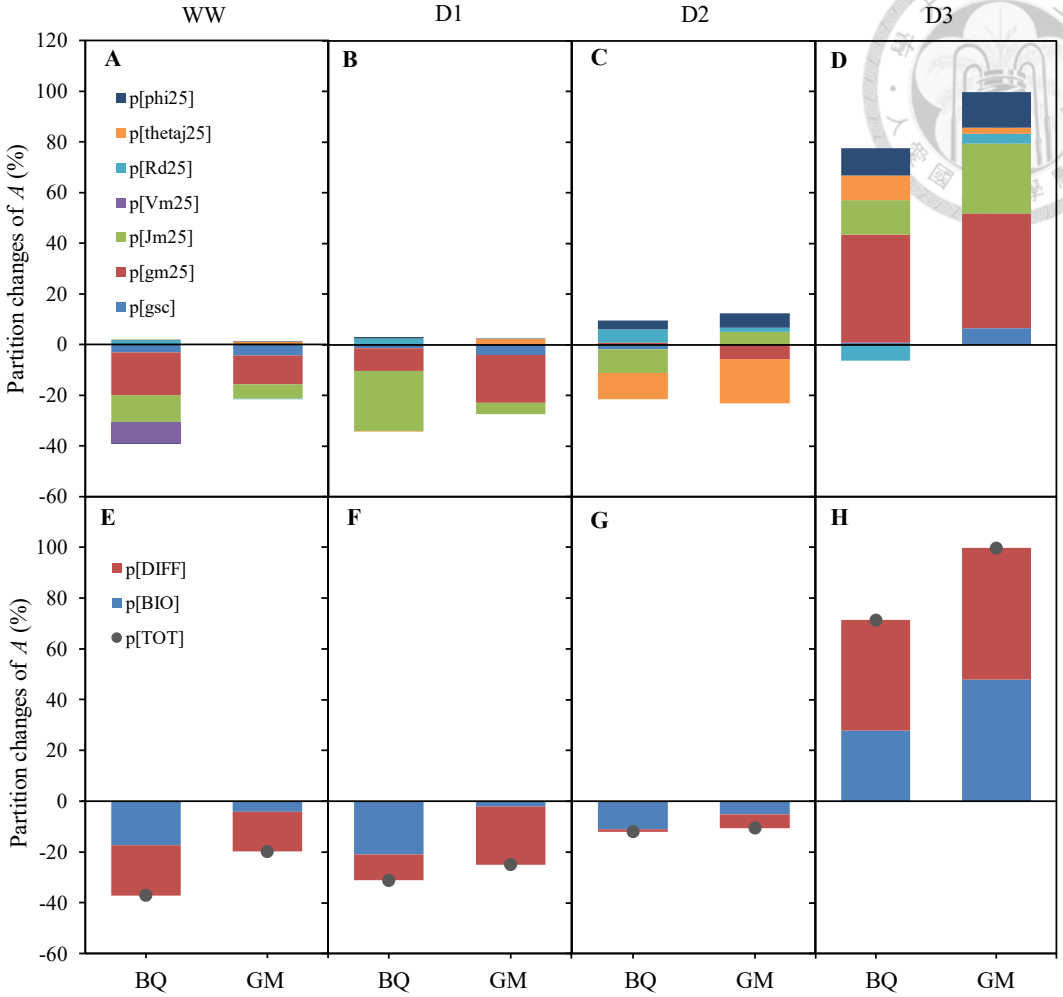

Fig. 3.10. The contribution of gas exchange variables to the changes of *A* in 'Black Queen' (BQ), 'Golden Muscat' (GM) compare with 'Riesling' under various drought conditions. Leaf gas exchange of vines was measured at25°C, light intensity 1200 μmol·m^{-2}·s^{-1}. **A-D** p[*x*] indicate the contribution of variable *x* to *A*. p[phi]=initial slope of electron transport rate versus light (φ); p[thetaj]=convexity factor of electron transport rate versus light; p[Rd]=day respiration rate, (R_d); p[Jm]=maximum electron transport capacity at saturating light (J_{max}); p[gm]=mesophyll conductance (g_m); p[gsc]=CO_2 stomatal conductance (g_{sc}). **E-H** shows total change of *A* (p[TOT]), contribution of biochemical factors (p[BIO]=p[phi]+ p[thetaj]+p[Rd]+p[Jm]) and diffusional factors (p[DIFF]=p[gm]+p[gsc]). WW, well-watered condition; D1, slight stress; D2, moderate stressed; D3, extreme stress.

doi:10.6342/NTU202400535

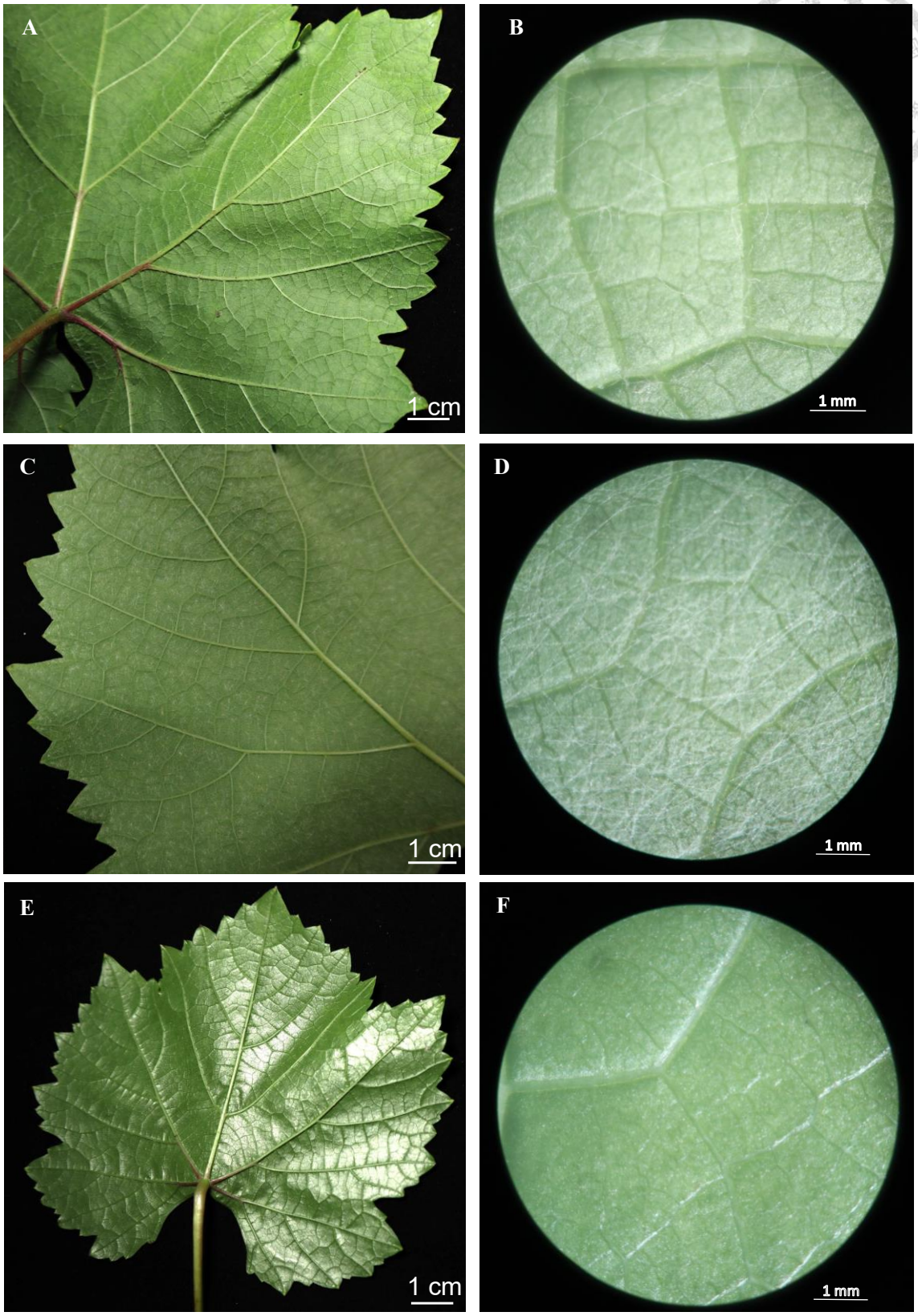

Fig. 3.11. Leaf back of the grape cultivars (**A**, **C**, and **E**) and 30X magnified under the dissecting microscope (**B**, **D**, and **F**). **A** and **B:** 'Black Queen'; **C** and **D**: 'Golden Muscat'; **E** and **F**: 'Riesling'.

doi:10.6342/NTU202400535

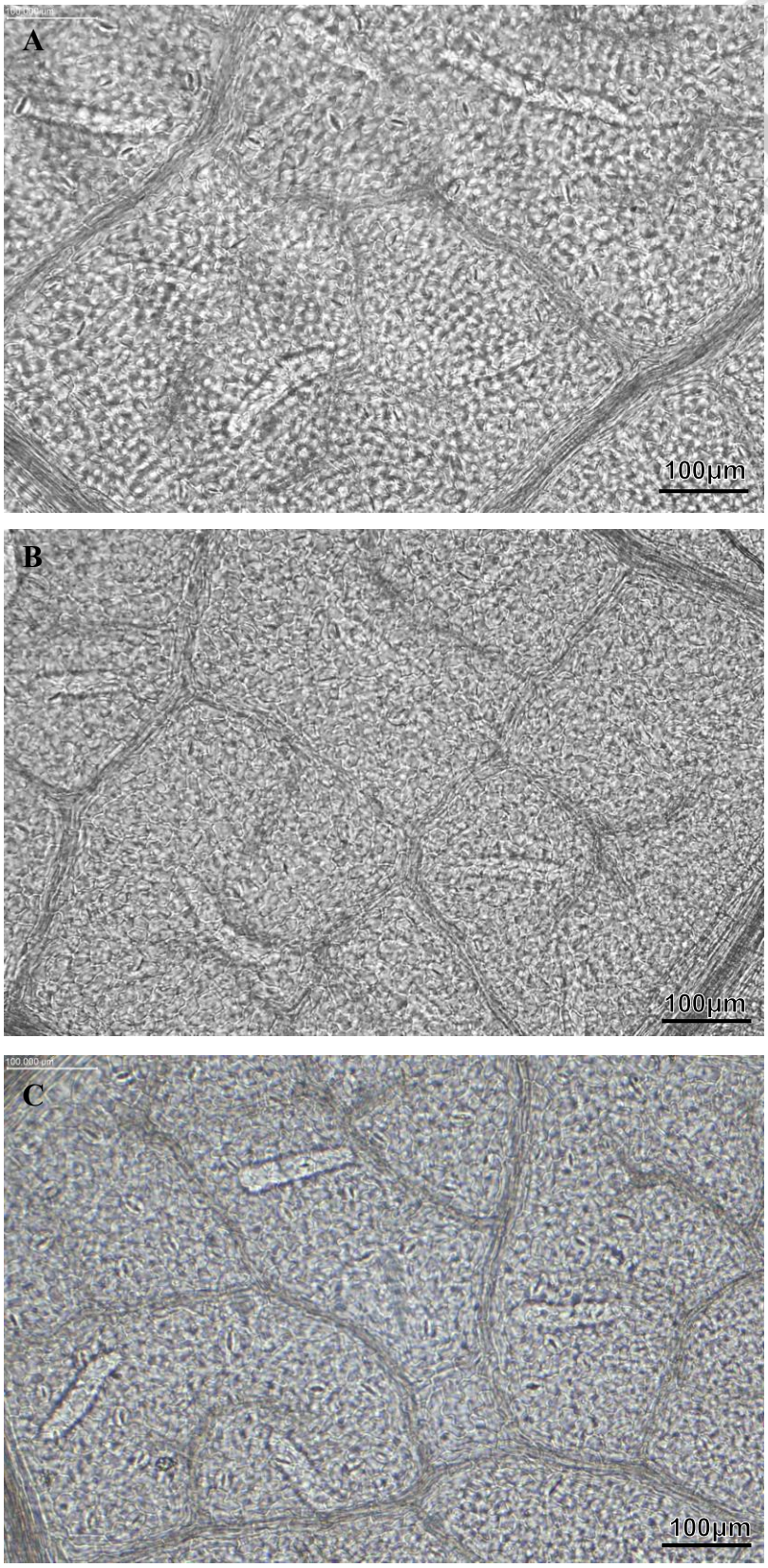

Fig. 3.12. The abaxial side of ‘Black Queen’ (**A**), ‘Golden Muscat’ (**B**), and ‘Riesling’ (**C**) with 100X magnified by cleaning technique.

doi:10.6342/NTU202400535

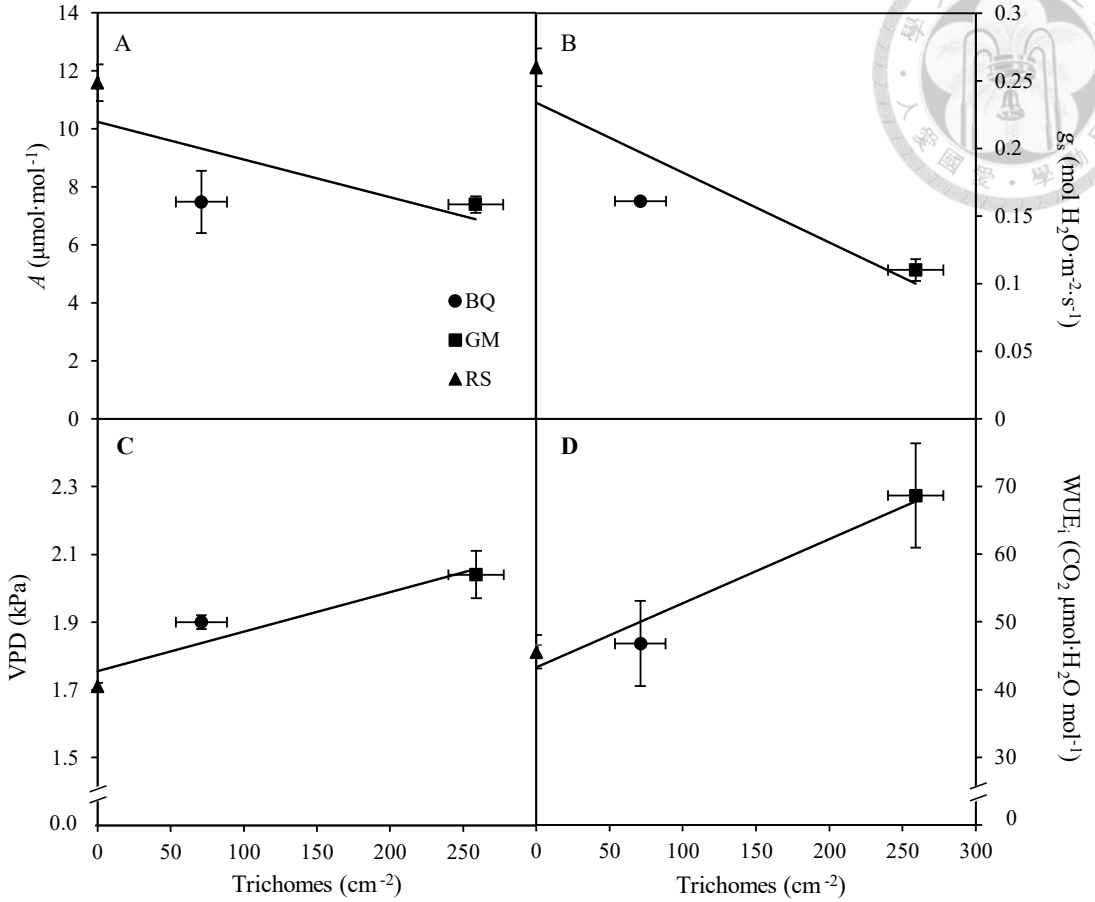

Fig. 3.13. Functions of (**A**) photosynthetic assimilation rate (*A*), (**B**) stomata conductance (g_s) (C) vapor pressure deficient based on leaf temperature (VPD) and (**D**) intrinsic water use efficiency (WUE_i) against trichomes in 'Black Queen' ('BQ'), 'Golden Muscat' ('GM') and 'Riesling' ('RS') grape leaves. Gas exchange data was taken from table 3.1 in well-watered condition, and trichome densities were taken from table 3.10. Each data show as mean with stander error (n=3). A = -0.013trichome + 10.249, r=0.724. g_s = -0.0005trichome + 0.2338, r=0.820. VPD = 0.0012trichome + 1.7551, r=0.942. WUE_i = 0.0947trichome + 43.258, r = 0.975.

doi:10.6342/NTU202400535

Chapter 4. Discussion

4.1. Gas exchange behaviors of grapes under well-water condition

In both experiments, A at saturated light of vinifera grape 'Riesling' (*Vitis vinifera*, 'RS') was greater than that of hybrid cultivars (*V. vinifera* X *V. labrusca*), 'Golden Muscat' ('GM') and 'Black Queen' ('BQ'), under well-watered conditions (Table 3.1 and Table 3.5). According to the measurement and *FvCB* modeling results (Table 3.1,3.2, 3.5 and Table 3.7), 'RS' also had higher g_s, ϕ_{PSII}, g_m, and J_{max}. A higher A of *V. vinifera* compared with *V. labrusca* has been reported (Patakas et al., 2003). Although in experiment 1 (Exp.1), g_m was not different between the three cultivars, g_m was significantly higher in 'RS' than in the hybrid cultivars in the well-watered condition in the second experiment. The difference in g_m may be due to leaf anatomical differences, such as chloroplast surface area exposed to the intercellular airspaces per unit leaf area (S_c), cell wall thickness, and cell wall components (Clemente-Moreno et al., 2019; Knauer et al., 2022; Tomás Magdalena et al., 2013).

Moreover, scatter graph of g_m and A (Fig. 3.3 A.) showed that under a similar g_m, 'RS' had higher A, indicating that the biochemical process also played a major role in influencing the A of 'RS'. Compared with 'RS', the lower efficiency of A in hybrid cultivars was mainly caused by g_s, g_m, and J_{max} (Fig. 3.4). Among them, J_{max} was the dominant variable that made A of hybrid cultivars lower than 'RS' (Fig. 3.4). The significant difference in J_{max} between the three cultivars (Table 3.2) could be told from the light curves (Fig. 3.1) that A of 'RS' at saturating light intensity was superior to the two hybrid cultivars. The difference in A of grapes affected by J_{max} and g_s was reported by Greer (2018) who showed that not only diffusional factors (g_s and g_m) but also biochemical processes were important influences. Because the modeling method relied

doi:10.6342/NTU202400535

on ϕ_{PSII}, the low A of hybrid cultivars might be caused by its low ϕ_{PSII} at the well-watered conditions. The difference in J_{max} may also lie in the reduction of g_m, which restricts CO_2 activity at the chloroplast (Ethier and Livingston, 2004). In addition, the enzymes engaged in the RuBP regeneration process, Ru5PK and ATP synthesis, would limit the photosynthetic assimilation rate (Dias and Brüggemann, 2010; Tezara et al., 1999).

4.2. Gas exchange and *FvCB* variables at various water availability

The result of Exp. 1 demonstrated the importance of the biochemical parameters, particularly the relationship between J_{max} and A, and the variation in WUE_i between hybrid cultivars and vinifera grapes. The experiment 2 (Exp. 2) examined the gas exchange behavior of the three grape varieties to determine how biochemical processes and g_s, g_m affected the A under various water availability.

In Exp. 2, A and g_s of all three cultivars decreased as drought increased, whereas g_m and V_{cmax} remained consistent until the extreme drought was imposed (Fig 3.7 and Fig. 3.8). Flexas et al. (2009) showed that as the grapevines encountered drought conditions, A and g_s dropped immediately, while g_m decreased at the later stages. In Exp. 2, C_i decreased in the medium drought (D2) and increased in the extreme drought (Fig 3.7). Flexas et al. (2002) reported that the variation of C_i as the grapevines under the severe drought was one of the indicators of the limitation of g_m on A. The effect of g_m on the decrease in A was shown in the analysis of the contribution of the variables to the overall A under drought.

To understand the gas exchange behavior of each cultivar that underwent drought

doi:10.6342/NTU202400535

conditions, the means of the variables were modeled, and the changes in A were calculated using an integrated numerical method (Buckley and Diaz-Espejo, 2015). In 'BQ' and 'GM', A of vines at D3 was 70% less efficient than that of well-watered vines, while in 'RS' A of vines at D3 was 90% less efficient than well-watered vines (Fig. 3.9). Moreover, differences in A between the hybrid cultivars and 'RS' were reduced as drought increased (Fig. 3.10). Overall, 'GM' having the lowest C_i and highest WUE_i among the three cultivars at the well-water stages, performed the best A under extremely drought conditions (Table 3.5).

The partitioning result showed that as drought increased, the drop in A in the three cultivars was caused by g_s, g_m, and the biochemical factor J_{max}. The effect of diffusional factors (g_s and g_m) increased under drought in all three cultivars, which was consistent with previous studies showing that the resistance of g_s and g_m increased with drought (Flexas et al., 2009). g_m was related to the leaf lamina hydraulic conductance as the grapes were under drought conditions (Ferrio et al., 2012). Studies of the effect of aquaporins on g_s, g_m, and A revealed that water transportation affected CO_2 diffusion (Flexas et al., 2006). The production of apoplastic antioxidants, such as peroxidase, superoxide dismutase, and hydrogen peroxide, which are negatively related to g_m, can also explain the reduction in g_m under water stress (Clemente-Moreno et al., 2019).

In addition to g_s and g_m, the decrease in A with drought was highly influenced by J_{max} in all three cultivars (Fig. 3.9). In grapevines during drought conditions, J_{max} decreased but V_{cmax} remained consistent (de Souza et al., 2005). With no reduction in Ru5PK, the decrease in J_{max} might be caused by a reduction in ATP synthesis or CO_2 diffusion (de Souza et al., 2005). In addition, the modeling results from the numerical

doi:10.6342/NTU202400535

integration method showed that only the well-watered 'BQ' was limited by the Rubisco carboxylation process, and all other cultivars and water conditions were limited by RuBP (ribulose-1,5-bisphosphate) regeneration, which depends on the electron transportation rate. RuBP has been reported as the predominant *A* limitation in the *V. vinifera* 'Chardonnay' leaf (Greer, 2018). Studies have shown that RuBP regeneration limited the photosynthesis rate below 30℃ (Greer and Weedon, 2012). However, it has also been reported that *A* in grapevines is usually limited by Rubisco rather than the RuBP-related process (Flexas et al., 2002; Flexas et al., 2010). Under drought stress, the reduction in *A* was made by diffusional factor initially, and then the Rubisco activities and electron transportation were secondary reduced followed by the low g_s (Flexas et al., 2002). In addition to J_{max}, φ underwent clear alterations with increasing drought (Fig. 3.8), which led φ to a linear correlation with g_s and *A* in experiment 2 but not in experiment 1 (Table 3.3 and Table 3.9).

4.3. Relationship of intrinsic water use efficiency (WUE_i) and C_i to g_m and g_s

The changes in C_i and WUE_i did not follow the same pattern of the changes in g_s and *A* as drought increased (Fig 3.7). However, under the well-watered conditions, WUE_i showed a negative correlation with C_i, in which 'GM' had the lowest C_i and highest WUE_i (Fig. 3.4). The results in Exp. 2 (Table 3.9) showed a similar trend to the well-watered condition. The negative correlation of WUE_i to C_i can be described by the constant ambient CO_2 concentration (Bunce, 2016).

Despite WUE_i, C_i was highly correlated with g_m/g_s in both Exp. 1 and 2 (Table 3.3 and Table 3.9). In addition, the ratio of g_m to g_s was positively related to WUE_i. Scatter graph of WUE_i in g_m/g_s (Fig. 3.3 B.) showed that 'GM' distributed mainly at the higher

doi:10.6342/NTU202400535

end although ‘RS’ had high g_m and A. This relationship was the same as that in previous studies on grapevines (Flexas et al., 2010; Tomás M. et al., 2014), which indicates that an improvement in the g_m value would improve the water use of the plant as g_s constant. These relationships of g_m/g_s and C_i confirm that the improvement of C_i and g_m would be a possible approach to improve the photosynthetic response under water deficiency (Flexas et al., 2010).

4.4. Cultivar differences in the photosynthetic response

Several differences in the photosynthetic response between ‘RS’ and the two hybrid cultivars were observed in this study. During drought conditions, ‘GM’ maintain a similar C_i from WW to D3, while ‘RS’ had its highest C_i at D3 and ‘BQ’ had a decreasing C_i at D2. ϕ_{PSII} roughly declined with water deficient in ‘GM’ and ‘RS’, while ϕ_{PSII} did not show a significant decline in ‘BQ’, as it was already low at the WW stage. The difference in response in C_i and ϕ_{PSII} between the three cultivars (Fig 3.7) might lead to the different response in the g_m and biochemical processes. Moreover, the modeling result of the cultivars suffered drought indicated that the decreased A in hybrid cultivars was mainly caused by diffusional factors, while the decreased A in ‘RS’ was more contributed by biochemical factors (Fig. 3.9). The diffusional factors, especially for g_m, were the main contributors to the higher A of hybrid cultivars than ‘RS’ at extreme drought (Fig. 3.10). The difference not only happened between the hybrid cultivars and the *V. vinifera* ‘RS’ but also between the two hybrids ‘GM’ and ‘BQ’. From the well-watered stage to medium water deficiency (D2), the decreases in A in ‘GM’ were caused by diffusional factors, while in ‘BQ’ was mainly caused by biochemical factors (Fig. 3.9). In the first experiment, biochemical factors also contributed to most of the lower A efficiency in ‘BQ’ than in ‘RS’. In the two

doi:10.6342/NTU202400535

experiments, ‘GM’ had a relatively low g_s but similar stomata density (Table 3.10). Compared with the other two cultivars, ‘GM’ had better WUE_i and *A* under drought stress.

The photosynthetic difference between *V. labrusca* and *V. vinifera* has been reported on the gas conductance in the intercellular space, which was caused by the mesophyll structure and liquid conductance (Patakas et al., 2003). However, whether hybrid cultivars inherited the mesophyll structure of *V. labrusca* still need to be studied.

4.5. Trichome densities and gas exchange behavior

Table 3.10 showed that ‘GM’ had the highest trichome densities. The superior trichome density and better performance under drought of ‘GM’ was consistent with previous studies on olive (*Olea europaea* L.), *Arabidopsis lyrata*, and potato (*Solanum tuberosum* L.) that the presence of trichomes on leaves represented better drought tolerance (Boguszewska-Mańkowska et al., 2018; Boughalleb and Hajlaoui, 2011; Huttunen et al., 2010). In addition, the trichome densities were negatively related to g_s, and positively related to WUE_i in this study (Fig. 3.13), which were consistent with the studies on tomato (*Solanum lycopersicum*) (Galdon-Armero et al., 2018). The result of VPD positively related to trichome density was found by Schreuder et al. (2001) that the trichomes increased turbulence of the boundary layer and caused the high VPD, which further leaded the stomata close. However, in tomato, trichomes increased g_s (Gasparini et al., 2021), and Amada et al. (2017) reported that trichomes had small effects on gas exchange and WUE_i. In this study, the correlation between trichome densities and gas exchange variables were not significant due to the small sample size, which showed trichomes affected to the gas exchange in grapes need more study.

doi:10.6342/NTU202400535

Chapter 5 Conclusion

Two experiments in this thesis revealed the difference in gas exchange between *Vitis vinifera* 'Riesling' and hybrid cultivars (*V. vinifera* x *V. labrusca*) 'Black Queen' and 'Golden Muscat'. Under well-watered condition, the hybrid cultivars had lower photosynthesis assimilation rates than the vinifera 'Riesling', which was caused by their lower stomata conductance (g_s), mesophyll conductance (g_m), and maximum electron transport capacity at saturating light (J_{max}). However, 'Golden Muscat' showed a better intrinsic water use efficiency (WUE_i), g_m to g_s ratio, and low C_i at well-watered conditions. On the other hand, 'Golden Muscat' had a smaller decrease in A than 'Riesling' at extreme drought condition. This thesis revealed that the relationship between g_m/g_s and WUE_i was not only observed in vinifera grape but also in the hybrid cultivars. The maintenance of g_m in the hybrid cultivars under extreme drought conditions made hybrid cultivars a possible breeding material for the water stress tolerance. However, the effect of the leaves' trichomes and mesophyll structure on the gas exchange of grape leaves remains to be studied.

doi:10.6342/NTU202400535

References

Council of Agriculture, Executive Yuan. 2021. Production value of grapes in Taiwan. <https://agrstat.coa.gov.tw/sdweb/public/inquiry/InquireAdvance.aspx>.

Agrawal, A.A., M. Fishbein, R. Jetter, J.P. Salminen, J.B. Goldstein, A.E. Freitag, and J.P. Sparks. 2009. Phylogenetic ecology of leaf surface traits in the milkweeds (*Asclepias* spp.): chemistry, ecophysiology, and insect behavior. New Phytol. 183:848-867.

Amada, G., Y. Onoda, T. Ichie, and K. Kitayama. 2017. Influence of leaf trichomes on boundary layer conductance and gas-exchange characteristics in *Metrosideros polymorpha* (Myrtaceae). Biotropica 49:482-492.

Benz, B.W. and C.E. Martin. 2006. Foliar trichomes, boundary layers, and gas exchange in 12 species of *epiphytic Tillandsia* (Bromeliaceae). J. Plant Physiol. 163:648-656.

Bernacchi, C.J., A.R. Portis, H. Nakano, S. von Caemmerer, and S.P. Long. 2002. Temperature response of mesophyll conductance. Implications for the determination of Rubisco enzyme kinetics and for limitations to photosynthesis in *Vivo*. Plant Physiol. 130:1992-1998.

Boguszewska-Mańkowska, D., M. Pieczyński, A. Wyrzykowska, H.M. Kalaji, L. Sieczko, Z. Szweykowska-Kulińska, and B. Zagdańska. 2018. Divergent strategies displayed by potato (*Solanum tuberosum* L.) cultivars to cope with soil drought. J. Agron. Crop Sci. 204:13-30.

Bota, B.J., J. Flexas, and H. Medrano. 2001. Genetic variability of photosynthesis and water use in Balearic grapevine cultivars. Ann. Appl. Biol. 138:353-361.

Boughalleb, F. and H. Hajlaoui. 2011. Physiological and anatomical changes induced by drought in two olive cultivars (cv Zalmati and Chemlali). Acta Physiol. Plant

doi:10.6342/NTU202400535

33:53-65.

Buckley, T.N. and A. Diaz-Espejo. 2015. Partitioning changes in photosynthetic rate into contributions from different variables. Plant Cell Environ. 38:1200-1211.

Caemmerer, S. 2000. Biochemical models of leaf photosynthesis. CSIRO, Collingwood, Australia.

Chaves, M.M., T.P. Santos, C.R. Souza, M.F. Ortuño, M.L. Rodrigues, C.M. Lopes, J.P. Maroco, and J.S. Pereira. 2007. Deficit irrigation in grapevine improves water-use efficiency while controlling vigour and production quality. Ann. Appl. Biol. 150:237-252.

Chen, T.-W., M. Henke, P.H.B. De Visser, G. Buck-Sorlin, D. Wiechers, K. Kahlen, and H. Stützel. 2014. What is the most prominent factor limiting photosynthesis in different layers of a greenhouse cucumber canopy? Ann. Bot. 114:677-688.

Clemente-Moreno, M.J., J. Gago, P. Diaz-Vivancos, A. Bernal, E. Miedes, P. Bresta, G. Liakopoulos, A.R. Fernie, J.A. Hernandez, and J. Flexas. 2019. The apoplastic antioxidant system and altered cell wall dynamics influence mesophyll conductance and the rate of photosynthesis. Plant J. 99:1031-1046.

da Silva, J.R., A.E. Patterson, W.P. Rodrigues, E. Campostrini, and K.L. Griffin. 2017. Photosynthetic acclimation to elevated CO_2 combined with partial rootzone drying results in improved water use efficiency, drought tolerance and leaf carbon balance of grapevines (*Vitis labrusca*). Environ. Exp. Bot. 134:82-95.

de Souza, C.R., J.P. Maroco, T.P. dos Santos, M.L. Rodrigues, C. Lopes, J.S. Pereira, and M.M. Chaves. 2005. Control of stomatal aperture and carbon uptake by deficit irrigation in two grapevine cultivars. Agric. Ecosyst. Environ. 106:261-274.

Dias, M.C. and W. Brüggemann. 2010. Limitations of photosynthesis in *Phaseolus*

doi:10.6342/NTU202400535

vulgaris under drought stress: gas exchange, chlorophyll fluorescence and Calvin cycle enzymes. Photosynthetica 48:96-102.

Ehleringer, J., O. Björkman, and H.A. Mooney. 1976. Leaf pubescence: effects on absorptance and photosynthesis in a desert shrub. Science 192:376-377.

Ennajeh, M., A.M. Vadel, H. Cochard, and H. Khemira. 2010. Comparative impacts of water stress on the leaf anatomy of a drought-resistant and a drought-sensitive olive cultivar. J. Hortic. Sci. Biotechnol. 85:289-294.

Ethier, G.J. and N.J. Livingston. 2004. On the need to incorporate sensitivity to CO_2 transfer conductance into the Farquhar-von Caemmerer-Berry leaf photosynthesis model. Plant Cell Environ. 27:137-153.

Evans, J.R., T.D. Sharkey, J.A. Berry, and G.D. Farquhar. 1986. Carbon isotope discrimination measured concurrently with gas exchange to investigate CO_2 diffusion in leaves of higher plants. Funct. Plant Biol. 13:281-292.

FAO. 2017. The future of food and agriculture- Trends and challenges. United Nations, Rome.

FAO, United Nations. 2021. Production of grapes. <https://www.fao.org/faostat/en/#data/QCL>.

Farquhar, G.D. and T.D. Sharkey. 1982. Stomatal conductance and photosynthesis. Annu. Rev. Plant Physiol. 33:317-345.

Farquhar, G.D. and T.D. Sharkey. 1994. Photosynthesis and carbon assimilation, p. 187-210. In: K.J. Boote, J.M. Bennett, T.R. Sinclair, and G.M. Paulsen (eds.). Physiology and determination of crop yield. American Society of Agronomy, Madison, Wisconsin, USA.

Farquhar, G.D., S. von Caemmerer, and J.A. Berry. 1980. A Biochemical model of photosynthetic CO_2 assimilation in leaves of C_3 species. Planta 149:78-90.

doi:10.6342/NTU202400535

Ferrio, J.P., A. Pou, I. Florez-Sarasa, A. Gessler, N. Kodama, J. Flexas, and M. Ribas-Carbo. 2012. The Peclet effect on leaf water enrichment correlates with leaf hydraulic conductance and mesophyll conductance for CO_2. Plant Cell Environ. 35:611-625.

Flexas, J., M. Barón, J. Bota, J.M. Ducruet, A. Gallé, J. Galmés, M. Jimenéz, A. Pou, M. Ribas-Carbo, C. Sajnani, M. Tomás, and H. Medrano. 2009. Photosynthesis limitations during water stress acclimation and recovery in the drought-adapted *Vitis* hybrid Richter-110 (*V. berlandieri*x*V.rupestris*). J. Exp. Bot 60:2361-2377.

Flexas, J., J. Bota, J.M. Escalona, B. Sampol, and H. Medrano. 2002. Effects of drought on photosynthesis in grapevines under field conditions: An evaluation of stomatal and mesophyll limitations. Funct. Plant Biol. 29:461-471.

Flexas, J., J.M. Escalona, and H. Medrano. 1999. Water stress induces different levels of photosynthesis and electron transport rate regulation in grapevines. Plant Cell Environ. 22:39-48.

Flexas, J., J. Galmes, A. Galle, J. Gulias, A. Pou, M. Ribas-Carbo, M. Tomas, and H. Medrano. 2010. Improving water use efficiency in grapevines: potential physiological targets for biotechnological improvement. Aust. J. Grape Wine Res. 16:106-121.

Flexas, J., M. Ribas-Carbó, D.T. Hanson, J. Bota, B. Otto, J. Cifre, N. Mcdowell, H. Medrano, and R. Kaldenhoff. 2006. Tobacco aquaporin NtAQP1 is involved in mesophyll conductance to CO_2 *in vivo*. Plant J. 48:427-439.

Florez-Sarasa, I., M.J. Clemente-Moreno, J. Cifre, M. Capo, M. Llompart, A.R. Fernie, and J. Bota. 2020. Differences in metabolic and physiological responses between local and widespread grapevine cultivars under water deficit stress. Agronomy 10:1052.

doi:10.6342/NTU202400535

Galdon-Armero, J., M. Fullana-Pericas, P.A. Mulet, M.A. Conesa, C. Martin, and J. Galmes. 2018. The ratio of trichomes to stomata is associated with water use efficiency in *Solanum lycopersicum* (tomato). Plant J. 96:607-619.

Galle, A., I. Florez-Sarasa, M. Tomas, A. Pou, H. Medrano, M. Ribas-Carbo, and J. Flexas. 2009. The role of mesophyll conductance during water stress and recovery in tobacco (*Nicotiana sylvestris*): acclimation or limitation? J. Exp. Bot 60:2379-2390.

Gasparini, K., M.F. Da Silva, L.C. Costa, S.C.V. Martins, D.M. Ribeiro, L.E.P. Peres, and A. Zsögön. 2021. The Lanata trichome mutation increases stomatal conductance and reduces leaf temperature in tomato. J. Plant Physiol. 260:153413.

Genty, B., J.-M. Briantais, and N.R. Baker. 1989. The relationship between the quantum yield of photosynthetic electron transport and quenching of chlorophyll fluorescence. Biochim. Biophys. Acta 990:87-92.

Grassi, G. and F. Magnani. 2005. Stomatal, mesophyll conductance and biochemical limitations to photosynthesis as affected by drought and leaf ontogeny in ash and oak trees. Plant Cell Environ. 28:834-849.

Greer, D.H. 2018. The short-term temperature-dependency of CO_2 photosynthetic responses of two *Vitis vinifera* cultivars grown in a hot climate. Environ. Exp. Bot. 147:125-137.

Greer, D.H. and M.M. Weedon. 2012. Modelling photosynthetic responses to temperature of grapevine (*Vitis vinifera* cv. Semillon) leaves on vines grown in a hot climate. Plant Cell Environ. 35:1050-1064.

Guan, X.Q., S.J. Zhao, D.Q. Li, and H.R. Shu. 2004. Photoprotective function of photorespiration in several grapevine cultivars under drought stress.

doi:10.6342/NTU202400535

Photosynthetica 42:31-36.

Guerfel, M., O. Baccouri, D. Boujnah, W. Chaïbi, and M. Zarrouk. 2009. Impacts of water stress on gas exchange, water relations, chlorophyll content and leaf structure in the two main Tunisian olive (*Olea europaea* L.) cultivars. Sci. Hortic. 119:257-263.

Harley, P.C., F. Loreto, G. Di Marco, and T.D. Sharkey. 1992. Theoretical considerations when estimating the mesophyll conductance to CO_2 flux by analysis of the response of photosynthesis to CO_2. Plant Physiol. 98:1429-1436.

Harley, P.C., R.B. Thomas, J.F. Reynolds, and B.R. Strain. 1992. Modelling photosynthesis of cotton grown in elevated CO_2. Plant Cell Environ. 15:271-282.

Huttunen, P., K. Karkkainen, G. Loe, P. Rautio, and J. Agren. 2010. Leaf trichome production and responses to defoliation and drought in *Arabidopsis lyrata* (Brassicaceae). Ann. Bot. Fennici 47:199-207.

Ichie, T., Y. Inoue, N. Takahashi, K. Kamiya, and T. Kenzo. 2016. Ecological distribution of leaf stomata and trichomes among tree species in a Malaysian lowland tropical rain forest. J. Plant Res. 129:625-635.

Johnson, H.B. 1975. Plant pubescence: An ecological perspective. Bot. Rev. 41:233-258.

Jones, H.G. 1985. Partitioning stomatal and non-stomatal limitations to photosynthesis. Plant Cell Environ. 8:95-104.

Keller, M. 2010. The science of grapevines: Anatomy and physiology. Academic Press, Burlington, MA, USA.

Kenzo, T., R. Yoneda, M.A. Azani, and N.M. Majid. 2008. Changes in leaf water use after removal of leaf lower surface hairs on *Mallotus macrostachyus*

doi:10.6342/NTU202400535

(Euphorbiaceae) in a tropical secondary forest in Malaysia. J. For. Res. 13:137-142.

Knauer, J., M. Cuntz, J.R. Evans, Ü. Niinemets, T. Tosens, L.L. Veromann-Jürgenson, C. Werner, and S. Zaehle. 2022. Contrasting anatomical and biochemical controls on mesophyll conductance across plant functional types. New Phytol. 236:357-368.

Kok, B. 1948. A critical consideration of the quantum yield of *Chlorella* photosynthesis. Enzymologia 13:1-56.

Kono, A., Y. Ban, N. Mitani, H. Fujii, S. Sato, K. Suzaki, A. Azuma, N. Onoue, and A. Sato. 2018. Development of SSR markers linked to QTL reducing leaf hair density and grapevine downy mildew resistance in *Vitis vinifera*. Mol. Breeding 38:138.

Kortekamp, A. and E. Zyprian. 1999. Leaf hairs as a basic protective barrier against downy mildew of grape. J. Phytopathol. 147:453-459.

Laisk, A.K. 1977. Kinetics of photosynthesis and photorespiration of C_3 in plants. [In Russ.] Nauka, Moscow

Loreto, F., P.C. Harley, G. Di Marco, and T.D. Sharkey. 1992. Estimation of mesophyll conductance to CO_2 flux by three different methods. Plant Physiol. 98:1437-1443.

Martinez-Luscher, J., F. Morales, S. Delrot, M. Sanchez-Diaz, E. Gomes, J. Aguirreolea, and I. Pascual. 2015. Characterization of the adaptive response of grapevine (cv. Tempranillo) to UV-B radiation under water deficit conditions. Plant Sci. 232:13-22.

Maul, E., Institute for Grapevine Breeding Geilweilerhof. 2023. VIVC. 2023. <www.vivc.de>.

doi:10.6342/NTU202400535

Moualeu-Ngangue, D.P., T.-W. Chen, and H. Stützel. 2017. A new method to estimate photosynthetic parameters through net assimilation rate–intercellular space CO_2 concentration (A-C_i) curve and chlorophyll fluorescence measurements. New Phytol. 213:1543-1554.

OIV. 2019. 2019 Statistical report on world vitiviniculture. 2022. <https://www.oiv.int/public/medias/6782/oiv-2019-statistical-report-on-world-vitiviniculture.pdf>.

Olsovska, K., M. Kovar, M. Brestic, M. Zivcak, P. Slamka, and H.B. Shao. 2016. Genotypically identifying wheat mesophyll conductance regulation under progressive drought stress. Front. Plant Sci. 7.

Patakas, A., B. Noitsakis, and A. Chouzouri. 2005. Optimization of irrigation water use in grapevines using the relationship between transpiration and plant water status. Agric. Ecosyst. Environ. 106:253-259.

Patakas, A., D. Stavrakas, and I. Fisarakis. 2003. Relationship between CO_2 assimilation and leaf anatomical characteristics of two grapevine cultivars. Agronomie 23:293-296.

Perez-Estrada, L.B., Z. Cano-Santana, and K. Oyama. 2000. Variation in leaf trichomes of *Wigandia urens*: environmental factors and physiological consequences. Tree Physiol. 20:629-632.

Perez-Martin, A., J. Flexas, M. Ribas-Carbo, J. Bota, M. Tomas, J.M. Infante, and A. Diaz-Espejo. 2009. Interactive effects of soil water deficit and air vapour pressure deficit on mesophyll conductance to CO_2 in *Vitis vinifera* and *Olea europaea*. J. Exp. Bot 60:2391-2405.

Pons, T.L., J. Flexas, S. von Caemmerer, J.R. Evans, B. Genty, M. Ribas-Carbo, and E. Brugnoli. 2009. Estimating mesophyll conductance to CO_2: methodology,

doi:10.6342/NTU202400535

potential errors, and recommendations. J. Exp. Bot 60:2217-2234.

Salazar-Parra, C., J. Aguirreolea, M. Sanchez-Diaz, J.J. Irigoyen, and F. Morales. 2012. Photosynthetic response of Tempranillo grapevine to climate change scenarios. Ann. Appl. Biol. 161:277-292.

Salazar-Parra, C., I. Aranjuelo, I. Pascual, G. Erice, A. Sanz-Saez, J. Aguirreolea, M. Sanchez-Diaz, J.J. Irigoyen, J.L. Araus, and F. Morales. 2015. Carbon balance, partitioning and photosynthetic acclimation in fruit-bearing grapevine (*Vitis vinifera* L. cv. Tempranillo) grown under simulated climate change (elevated CO_2, elevated temperature and moderate drought) scenarios in temperature gradient greenhouses. J. Plant Physiol. 174:97-109.

Schreuder, M.D.J., C.A. Brewer, and C. Heine. 2001. Modelled influences of non-exchanging trichomes on leaf boundary layers and gas exchange. J. Theor. Biol. 210:23-32.

Schuepp, P.H. 1993. Tansley Review No. 59 Leaf boundary layers. New Phytol. 125:477-507.

Sharkey, T.D. 1985. Photosynthesis in intact leaves of C_3 plants: Physics, physiology and rate limitations. Bot. Rev. 51:53-105.

Sharkey, T.D. 2016. What gas exchange data can tell us about photosynthesis. Plant Cell Environ. 39:1161-1163.

Sharkey, T.D., C.J. Bernacchi, G.D. Farquhar, and E.L. Singsaas. 2007. Fitting photosynthetic carbon dioxide response curves for C_3 leaves. Plant Cell Environ. 30:1035-1040.

Silim, S.N., N. Ryan, and D.S. Kubien. 2010. Temperature responses of photosynthesis and respiration in *Populus balsamifera* L.: Acclimation versus adaptation. Photosyn. Res. 104:19-30.

doi:10.6342/NTU202400535

Sun, Y., L. Gu, R.E. Dickinson, S.G. Pallardy, J. Baker, Y. Cao, F.M. Damatta, X. Dong, D. Ellsworth, D. Van Goethem, A.M. Jensen, B.E. Law, R. Loos, S.C.V. Martins, R.J. Norby, J. Warren, D. Weston, and K. Winter. 2014. Asymmetrical effects of mesophyll conductance on fundamental photosynthetic parameters and their relationships estimated from leaf gas exchange measurements. Plant Cell Environ. 37:978-994.

Tezara, W., V.J. Mitchell, S.D. Driscoll, and D.W. Lawlor. 1999. Water stress inhibits plant photosynthesis by decreasing coupling factor and ATP. Nature 401:914-917.

Thitz, P., B.J.H.M. Possen, E. Oksanen, L. Mehtätalo, V. Virjamo, and E. Vapaavuori. 2017. Production of glandular trichomes responds to water stress and temperature in silver birch (*Betula pendula*) leaves. Can. J. For. Res. 47:1075-1081.

Tomás, M., J. Flexas, L. Copolovici, J. Galmés, L. Hallik, H. Medrano, M. Ribas-Carbó, T. Tosens, V. Vislap, and Ü. Niinemets. 2013. Importance of leaf anatomy in determining mesophyll diffusion conductance to CO_2 across species: quantitative limitations and scaling up by models. J. Exp. Bot 64:2269-2281.

Tomás, M., H. Medrano, E. Brugnoli, J.M. Escalona, S. Martorell, A. Pou, M. Ribas-Carbó, and J. Flexas. 2014. Variability of mesophyll conductance in grapevine cultivars under water stress conditions in relation to leaf anatomy and water use efficiency. Aust. J. Grape Wine Res. 20:272-280.

Tzortzakis, N., A. Chrysargyris, and A. Aziz. 2020. Adaptive response of a native mediterranean grapevine cultivar upon short-term exposure to drought and heat stress in the context of climate change. Agronomy 10:249.

Vasco, A., M. Thadeo, M. Conover, and D.C. Daly. 2014. Preparation of samples for

doi:10.6342/NTU202400535

leaf architecture studies, a method for mounting cleared leaves. Appl. Plant Sci. 2:1400038.

Walker, B.J. and D.R. Ort. 2015. Improved method for measuring the apparent CO_2 photocompensation point resolves the impact of multiple internal conductances to CO_2 to net gas exchange. Plant Cell Environ. 38:2462-2474.

Weil, R.R. and N.C. Brady. 2017. Soil water: Characteristics and behavior, p. 207-250. In: D. Fox (ed.). The nature and properties of soils. Pearson Education, Essex, U.K.

Werker, E. 2000. Trichome diversity and development. Adv. Bot. Res. 31:1-35.

Wilson, K.B., D.D. Baldocchi, and P.J. Hanson. 2000. Quantifying stomatal and non-stomatal limitations to carbon assimilation resulting from leaf aging and drought in mature deciduous tree species. Tree Physiol. 20:787-797.

Yang, Y.-S. 2005. Grapes, p. 217-226. In: Council of Agriculture, Executive Yuan (ed.). Taiwan agriculture encyclopedia. Council of Agriculture, Executive Yuan, Taipei.

Yin, X., P.C. Struik, P. Romero, J. Harbinson, J.B. Evers, P.E.L. Van Der Putten, and J. Vos. 2009. Using combined measurements of gas exchange and chlorophyll fluorescence to estimate parameters of a biochemical C_3 photosynthesis model: a critical appraisal and a new integrated approach applied to leaves in a wheat (*Triticum aestivum*). Plant Cell Environ. 32:448-464.

Yin, X., Z. Sun, P.C. Struik, and J. Gu. 2011. Evaluating a new method to estimate the rate of leaf respiration in the light by analysis of combined gas exchange and chlorophyll fluorescence measurements. J. Exp. Bot 62:3489-3499.

Zufferey, V., J.L. Spring, T. Verdenal, A. Dienes, S. Belcher, F. Lorenzini, C. Koestel, J. Rosti, K. Gindro, J. Spangenberg, and O. Viret. 2017. Influence of water stress

doi:10.6342/NTU202400535

on plant hydraulics, gas exchange, berry composition and quality of Pinot noir wines in Switzerland. Oeno One 51:37-57.

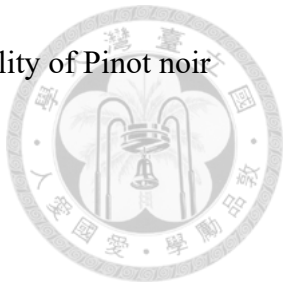

doi:10.6342/NTU202400535

Appendix

Appendix 1. Rubisco kinetics value of tobacco (Nicotiana tabacum) from Walker and Ort (2015) for model fitting and values of c, ΔH_a, ΔH_d and ΔS for adjust parameters to adjust the variables to leaf temperature 25℃.

Rubisco kinetics	value at 25℃	c	ΔH_a	ΔH_d	ΔS
K_C (Pa)	27.24	35.98	80.99		
K_O (kPa)	16.58	12.38	23.72		
Γ^* (Pa)	3.74	11.89	24.46		
Temperature adjusting					
V_{cmax}		26.36	65.33		
J		17.71	43.90		
R_d		18.72	46.39		
g_m		20.01	49.60	437.40	1.40

doi:10.6342/NTU202400535